Journal of South American Earth Sciences 32 (2011) 75–95

Contents lists available at ScienceDirect

Journal of South American Earth Sciences

journal homepage: www.elsevier.com/locate/jsames

Alkaline magmatism in the Amambay area, NE Paraguay: The Cerro Sarambí complex

C.B. Gomes [a,*], V.F. Velázquez [b], R.G. Azzone [a], G.S. Paula [c]

[a] Institute of Geosciences, University of São Paulo, Rua do Lago 562, 05508-080 São Paulo, SP, Brazil
[b] Escola de Artes, Ciências e Humanidades, University of São Paulo, Rua Arlindo Bettio 1000, 03828-000 São Paulo, Brazil
[c] Geologist graduated at Institute of Geosciences, University of São Paulo, Brazil

ARTICLE INFO

Article history:
Received 24 September 2010
Accepted 12 April 2011

Keywords:
Alkaline magmatism
Geochemistry
Petrology
Amambay
Cerro Sarambí
Paraguay

ABSTRACT

The Early Cretaceous alkaline magmatism in the northeastern region of Paraguay (Amambay Province) is represented by stocks, plugs, dikes, and dike swarms emplaced into Carboniferous to Triassic-Jurassic sediments and Precambrian rocks. This magmatism is tectonically related to the Ponta Porã Arch, a NE-trending structural feature, and has the Cerro Sarambí and Cerro Chiriguelo carbonatite complexes as its most significant expressions. Other alkaline occurrences found in the area are the Cerro Guazú and the small bodies of Cerro Apuá, Arroyo Gasory, Cerro Jhú, Cerro Tayay, and Cerro Teyú. The alkaline rocks comprise ultramafic-mafic, syenitic, and carbonatitic petrographic associations in addition to lithologies of variable composition and texture occurring as dikes; fenites are described in both carbonatite complexes. Alkali feldspar and clinopyroxene, ranging from diopside to aegirine, are the most abundant minerals, with feldspathoids (nepheline, analcime), biotite, and subordinate Ti-rich garnet; minor constituents are Fe–Ti oxides and cancrinite as the main alteration product from nepheline. Chemically, the Amambay silicate rocks are potassic to highly potassic and have miaskitic affinity, with the non-cumulate intrusive types concentrated mainly in the saturated to undersaturated areas in silica syenitic fields. Fine-grained rocks are also of syenitic affiliation or represent more mafic varieties. The carbonatitic rocks consist dominantly of calciocarbonatites. Variation diagrams plotting major and trace elements vs. SiO_2 concentration for the Cerro Sarambí rocks show positive correlations for Al_2O_3, K_2O, and Rb, and negative ones for TiO_2, MgO, Fe_2O_3, CaO, P_2O_5, and Sr, indicating that fractional crystallization played an important role in the formation of the complex. Incompatible elements normalized to primitive mantle display positive spikes for Rb, La, Pb, Sr, and Sm, and negative for Nb–Ta, P, and Ti, as these negative anomalies are considerably more pronounced in the carbonatites. Chondrite-normalized REE patterns point to the high concentration of these elements and to the strong LRE/HRE fractionation. The Amambay rocks are highly enriched in radiogenic Sr and have T_{DM} model ages that vary from 1.6 to 1.1 Ga, suggesting a mantle source enriched in incompatible elements by metasomatic events in Paleo-Mesoproterozoic times. Data are consistent with the derivation of the Cerro Sarambí rocks from a parental magma of lamprophyric (minette) composition and suggest an origin by liquid immiscibility processes for the carbonatites.

1. Introduction

The Amambay Alkaline Province, located in the northeastern region of Eastern Paraguay at the border with Brazil (South Mato Grosso State), is made up of carbonatite-ring complexes (Cerro Sarambí and Cerro Chiriguelo) and several individual intrusions associated with the western flank of the Paraná basin (Fig. 1). This magmatic activity is believed to have been formed during the initial stages of rifting between Africa and South America in Early Cretaceous times.

The Amambay alkaline magmatism is tectonically controlled by the Ponta Porã Arch (Livieres and Quade, 1987), a prominent N35E-trending structural belt lying along a major gravity lineament oriented N55–60E in Eastern Paraguay and in the northern Chaco basin, at the west side of the Paraguay river. This trans-Paraguayan gravity lineament marks a possible structural zone related to older Precambrian tectonic events in the area (Comin-Chiaramonti et al., 1999). It intersects the Amambay depression, a tectonic feature aligned N40–45W, varying in width from about 40 to 70 km and extending over 300 km. On the Bouguer map, the Amambay depression, probably formed by sedimentary basins, is defined by three aligned gravity lows: Bella Vista in the north, the deepest

* Corresponding author. Tel.: +55 11 3091 4090; fax: +55 11 3091 4258.
E-mail address: cgomes@usp.br (C.B. Gomes).

0895-9811/$ – see front matter © 2011 Elsevier Ltd. All rights reserved.
doi:10.1016/j.jsames.2011.04.004

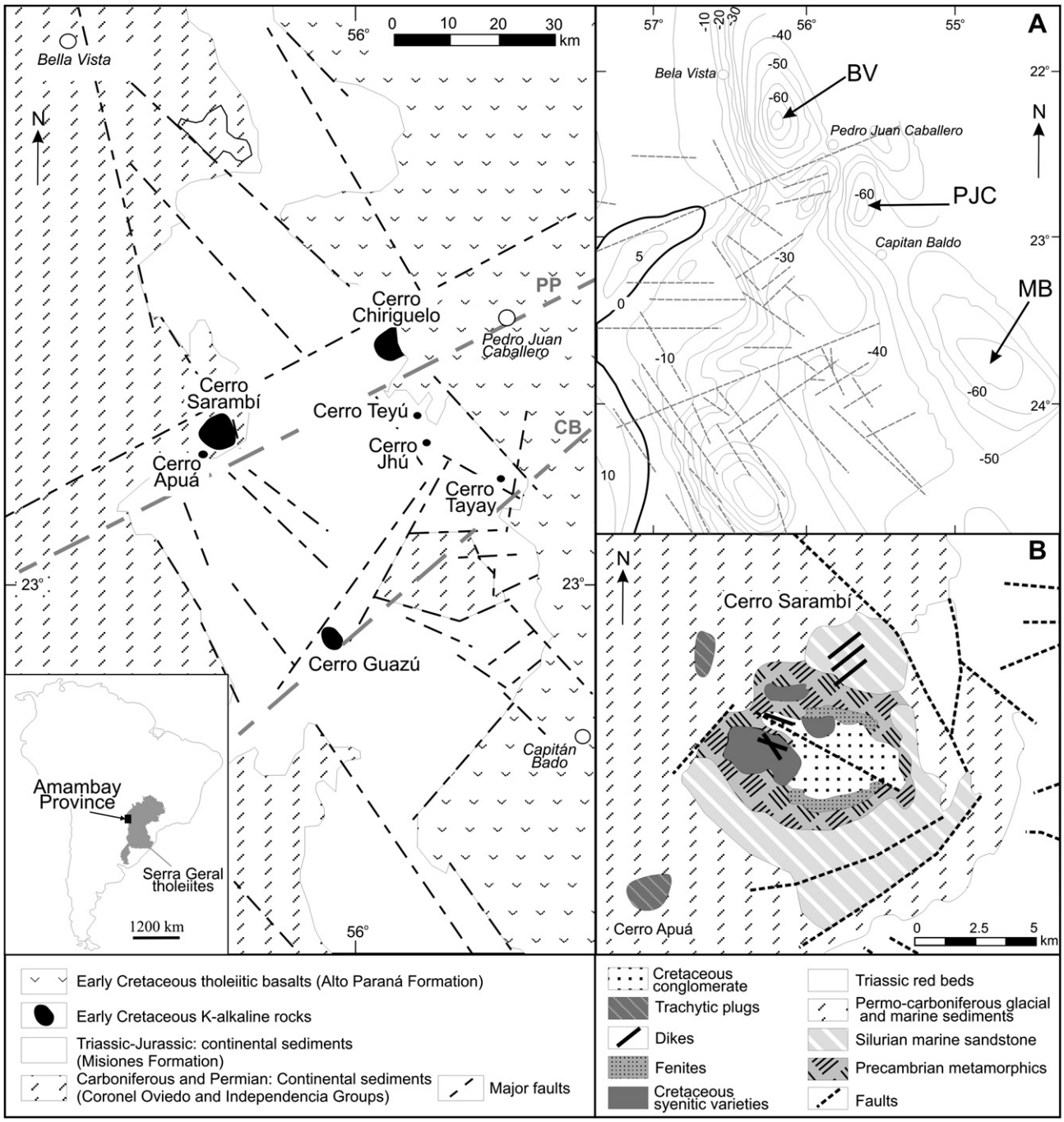

Fig. 1. Geographic distribution of alkaline occurrences in the Amambay Province, NE Paraguay (Comin-Chiaramonti et al., 1999). PP and CB, Ponta Porã and Capitán Bado tectonic lineaments, respectively (Livieres and Quade, 1987). Insets: A, Gravity lows of Bella Vista (BV), Pedro Juan Caballero (PJC) and Mbaracayú (MB) along the NW-trending Amambay rift belt (Comin-Chiaramonti et al., 1999, modified); B, Geological sketch map of the Cerro Sarambí (after Wiens, 1991, modified).

tectonic basin so far recognized in Eastern Paraguay; Pedro Juan Caballero at the center, the smallest of the three; and Mbaracayú in the south, the largest in this trend, 80 km long by 50–60 km wide (Fig. 1, inset A). The Amambay belt is poorly expressed by the mapped surface geology due to cover by Paraná flood tholeiites and Late Cretaceous Acaray sandstones. All known alkaline occurrences, including complexes, lava flows, plugs, and dikes, are situated within or on the boundaries of the Ponta Porã Arch where the Arch crosses the Amambay tectonic depression (Comin-Chiaramonti et al., 1999).

Thus, the Cerro Sarambí complex lies at the intersection of the Ponta Porã Arch with the Bella Vista fault zone, while satellite alkaline bodies southwest from that occurrence are spread along the Cerro Chiriguelo fault zone. The Cerro Chiriguelo complex is situated along the homonymous fault and close to a possible fault zone at the northeastern margin of the Bella Vista basin. Both Cerro Guazú and Cerro Tayay occur along the inferred fault that bounds the southeastern border of the Ponta Porã Arch. Hence, faults have exerted an important role in controlling the emplacement of alkaline magmas in the Amambay area, and the intersection of two major structural zones has greatly facilitated the process.

Also of great importance in the Amambay Province is the close association of the alkaline rocks and the Serra Geral flood tholeiites,

Table 1
Geochronological data for the Amambay alkaline rocks. Abbreviations: Ap, apatite; Bi, biotite; Ph, phlogopite; Ti, titanite; WR, whole rock; Ca, carbonatite; Gl, glimmerite; La, lamprophyre; Md, microdiorite; Py, pyroxenite; Sy, syenite; Tr, trachyte. References: 1) Comte and Hasui, 1971; 2) Eby and Mariano, 1986; 3) Eby and Mariano, 1992; 4) Sonoki and Garda, 1988; 5) Gibson et al., 1995; 6) Gibson et al., 2006; 7) Comin-Chiaramonti et al., 2007a; 8) Velázquez and Capaldi, unpublished data.

Locality	Rock type	Material	Age (Ma)	Mean age (Ma)	References
Fission-track					
Arroyo Gasory	Tr	Ti	146.7 ± 12.8		
	Tr	Ap	133.8 ± 11.6		
			134.1 ± 12.9	134.1 ± 2.4	3
Cerro Apuá	Tr	Ap	115.6 ± 11.6	114.8 ± 2.9	3
Cerro Chiriguelo	Ca	Ap	125.7 ± 12.9		3
	Ca	Ap	118.9 ± 20.3		
Cerro Guazú	La	Ap	114.0 ± 15.8		3
Cerro Sarambí	Py	Ap	110.8 ± 10.8	110.8 ± 2.8	3
	Py	Ap	111.5 ± 10.4		
	Ca	Ap	85.4 ± 4.6	86.3 ± 2.6	3
	Ca	Ap	87.2 ± 4.4		
K–Ar					
Arroyo Gasory	Tr	Bi	145 ± 8		2
	Tr	WR	137 ± 7		2
Cerro Chiriguelo	Md	Bi	146.7 ± 9.2		1, 4
	Md	WR	138.9 ± 20.3		1, 4
	Ca	Bi	128 ± 5		3
Cerro Guazú	La	Bi	117 ± 4		3
Cerro Sarambí	Sy	WR	140 ± 1		5
	Gl	WR	136 ± 9		8
Ar–Ar (plateau ages)					
Arroyo Gasory	Tr	Ph	142.92 ± 0.89		6
Cerro Chiriguelo	Tr	Bi	137.6 ± 0.7		7
Cerro Sarambí	La	Ph	142.88 ± 0.93		6
	La	Ph	142.89 ± 0.93		6
	Gl	Bi	139.3 ± 0.5		7

particularly in the area of Cerro Chiriguelo. There, geological evidence shows that the former rocks clearly predate the basalts. Despite the poor documentation (Table 1), which consists of radiometric determinations on biotite and whole rock samples (Comte and Hasui, 1971; Eby and Mariano, 1986, 1992; Sonoki and Garda, 1988; Gibson et al., 1995) and fission-track analyses on apatite and titanite (Eby and Mariano, 1992), the geochronological data confirm the field relationships. More recently, precise Ar–Ar determinations for the Early Cretaceous alkaline magmatism in the northeastern region of Paraguay, which also includes the Rio Apa Province at north of the country (Ar–Ar 138.7 ± 0.2 Ma, age result on biotite from a basanite dike cropping out near the city of Valle-mí), are reported in the literature. Plateau ages averaging 139 Ma (~143 Ma for phlogopite from Arroyo Gasory and Cerro Sarambí samples according to Gibson et al., 2006) were made available by Comin-Chiaramonti et al. (2007a) for biotite separates from a Cerro Sarambí glimmeritic vein and from a Cerro Chiriguelo trachytic lava flow, confirming that the Amambay alkaline magmatism was emplaced before the onset of the Early Cretaceous (Ar–Ar 134–133 Ma, cf. Thiede and Vasconcelos, 2008) Paraná-Angola-Etendeka flood volcanism.

This paper aims to provide better knowledge of the Cerro Sarambí complex based on mineral chemistry, geochemistry, and isotopic data of some rock types. It also provides general information on the other alkaline occurrences cropping out in the area.

2. Geology of the Cerro Sarambí

Cerro Sarambí, the largest Paraguayan alkaline complex, lies 60 km SW of the city of Pedro Juan Caballero at the border of Brazil and Paraguay. A geological sketch map after Wiens (1991) is shown in inset B of Fig. 1. The complex is circular, about 8.5 km in diameter, and was emplaced into Precambrian metamorphic rocks and domed Silurian and Permo-Carboniferous sediments (Haggerty and Mariano, 1983; Mariano and Druecker, 1985). It is composed mostly of an inner clinopyroxenite body, with minor aegirine-nepheline syenites. A large carbonatite core is presumably located in the center of the complex (Mariano, 1978). The intrusive rocks are crosscut by trachyte, phonolite, and lamprophyre dikes and by very thin veins and dikes of apatite–magnetite–calcite carbonatites (Eby and Mariano, 1992). Fenites are found as radial dikes penetrating the updomed country rock ridges in the southern rim of the alkaline intrusion (Gomes et al., 1996).

At least two isolated satellite plugs are recognized in the neighborhood of Cerro Sarambí (Wiens, 1991; Eby and Mariano, 1992; Paula, 2004). The first lies 2 km from the NW border of the complex and the second, also referred to as Cerro Apuá, is situated 4 km from its WSW limit. These occurrences are described as porphyritic trachytes, homogeneous in composition and consisting dominantly of phenocrysts of alkali feldspar with subordinate clinopyroxene, biotite, apatite, and titanite set in an aphanitic groundmass of alkali feldspar laths. Accessory minerals are magnetite and calcite.

3. Regional alkaline intrusions

A preliminary review of the alkaline magmatism in the Amambay area was presented by Gomes et al. (1996), with other geological characteristics given below.

In addition to Cerro Sarambí, Cerro Chiriguelo, also referred to as Cerro Corá in the literature, are the more outstanding expressions of the alkaline magmatism in the province, where additional occurrences are represented by the large intrusion of Cerro Guazú and the small bodies, formed mainly by plugs, lava flows, and dikes, of Cerro Apuá, Arroyo Gasory, Cerro Jhú, Cerro Tayay, and Cerro Teyú (Fig. 1). Except for Cerro Chiriguelo, which was the subject of geological and geophysical surveys for phosphate ore (Grossi-Sad, 1972; Mariano, 1978), the available information on those rocks is scarce and insufficient. In general they are emplaced into Paleozoic–Mesozoic sediments of continental origin ranging in age from Carboniferous (Coronel Oviedo Group) to Triassic-Jurassic (Misiones Formation), and Late Proterozoic metamorphic rocks.

The Cerro Chiriguelo complex is approximately circular with a diameter of 7.5 km and lies at 25 km WSW of the city of Pedro Juan Caballero. It intrudes into Precambrian metasedimentary rocks, with the surrounding ridges of country rocks updomed on the west, northwest, and southern rims; the southern and eastern rims are covered by late Paraná basalt flows (Haggerty and Mariano, 1983). According to Censi et al. (1989), the more common lithological types include alkaline silicate rocks, breccias with abundant Precambrian basement xenoliths (mainly quartzites and meta-arkoses), and carbonatites. The silicate rocks are represented mostly by massive fenites having a porphyritic texture and trachytic composition. The main carbonatite body, occupying the central parts of the intrusion, is elliptical, NE–SW-trending, with axes measuring about 600 × 300 m. The rock, usually subhedral-granular and medium to coarse-grained, shows exclusively calcite as carbonate phase. Accessory minerals are numerous and quite variable in composition. Alvikites, a hypoabissal carbonatitic rock showing typical aplitic texture, ferrocarbonatites and reomorphic fenites as dikes are scattered throughout the complex. Following Censi et al. (1989), at least three stages of carbonatite formation can be distinguished (calciocarbonatites — sovites and alvikites — and ferrocarbonatites).

In addition to Censi et al. (1989), the Cerro Chiriguelo was studied by Eby and Mariano (1986, 1992) and more recently underwent a comprehensive geochemical investigation by Castorina et al. (1996, 1997), Comin-Chiaramonti et al. (2005, 2007b), and Antonini et al. (2005), involving the complex's major, trace, and rare

Table 2
Representative analyses of clinopyroxenes from the Cerro Sarambí complex. FeO and Fe_2O_3 calculated following Droop (1987). Rock abbreviations: fen fenite; min, minette; mnsy, mela-nepheline syenite; nsy, nepheline syenite; ph, phonolite; pht, phonotephrite; sy, syenite; sd, syenodiorite; tr, trachyte; trph, tephriphonolite.

	Cerro Sarambí																Cerro Jhú		Cerro Teyú		Cerro Chiriguelo	
	Plutonic rocks							Dikes							Satellite plugs							
Sample	P41	P49	P46	P39	P68	P68	P43	P37	P37	P52	P52	P56	P61	P45	P34	P4	P10	P10	P17	P17	P28	P30
Rock type	mnsy	sd	sy	sy	nsy	nsy	fen	min	min	trph	trph	pht	pht	ph	tr	tr	trph	trph	trph	trph	fen	fen
SiO_2	47.77	52.46	51.44	52.43	52.42	52.97	53.53	52.81	53.87	51.73	52.36	50.99	52.31	52.67	52.03	50.56	51.52	48.40	50.58	50.41	52.44	51.22
TiO_2	1.15	0.65	0.46	0.57	0.53	0.71	1.14	0.69	0.69	0.71	0.65	1.07	3.18	0.31	0.49	0.44	0.44	0.57	0.39	0.39	0.23	1.43
Al_2O_3	4.70	1.10	0.75	0.90	0.75	1.01	1.08	1.13	0.85	1.27	1.21	1.85	1.53	1.27	1.45	2.70	1.26	4.00	1.50	1.54	0.44	0.52
Cr_2O_3	0.01	0.04	0.02	0.01				0.10	0.02			0.03	0.05	0.01		0.01		0.01				
ZrO_2	0.11		0.68	0.24	0.04	0.14	0.04	0.70		0.05	0.06	0.02	0.32	0.12	0.02	0.01		0.11	0.01	0.03	0.18	0.18
FeO_T	11.90	8.09	24.65	17.54	13.13	11.62	22.00	4.35	3.96	7.66	7.99	8.15	25.95	17.35	8.89	11.23	15.22	17.29	16.31	14.92	22.38	26.78
$FeO_{calc.}$	6.43	6.03	12.21	9.78	8.05	7.72	7.71	2.62	3.18	4.47	5.79	5.71	10.94	10.96	7.20	8.26	12.32	11.03	11.51	11.60	10.34	12.51
$Fe_2O_{3\ calc.}$	5.23	1.73	13.83	7.62	4.78	3.51	13.86	1.49	0.55	2.90	1.87	2.17	16.68	6.27	1.46	3.11	2.69	6.11	4.77	3.37	12.22	14.95
MnO	0.47	0.18	0.66	0.42	0.41	0.24	0.41	0.08	0.09	0.31	0.29	0.20	0.18	0.36	0.24	0.45	0.55	0.57	0.70	0.70	0.62	0.34
MgO	9.95	13.52	1.92	6.97	10.07	11.28	4.30	15.75	16.45	13.78	13.80	13.09	0.63	6.93	12.70	10.58	8.54	6.72	7.70	8.24	3.98	1.15
CaO	22.43	23.54	8.39	14.53	19.21	19.62	7.03	25.06	24.29	23.62	23.26	23.86	2.37	14.76	22.20	21.25	21.20	20.77	19.71	20.55	9.79	5.86
Na_2O	1.02	0.56	7.6	4.75	2.59	2.26	8.76	0.18	0.24	0.59	0.52	0.41	10.83	4.31	0.85	1.27	1.42	1.77	2.08	1.59	7.07	8.85
Total	99.27	99.82	97.96	98.22	98.86	99.46	97.86	100.62	100.23	99.42	99.81	99.40	99.02	97.97	98.64	98.64	99.94	100.06	98.94	98.42	97.30	97.00
Structural formulas calculated on the basis of 4 cations and 6 oxygens																						
Si	1.813	1.949	2.048	2.014	1.985	1.983	2.033	1.936	1.962	1.926	1.944	1.908	2.033	2.025	1.961	1.928	1.968	1.858	1.954	1.958	2.046	2.033
Al	0.187	0.048			0.015	0.017		0.049	0.036	0.056	0.053	0.082			0.039	0.072	0.032	0.142	0.046	0.042		
Fe^{3+}		0.003						0.015	0.001	0.018	0.003	0.010										
Sum T	2.000	2.000	2.048	2.014	2.000	2.000	2.033	2.000	2.000	2.000	2.000	2.000	2.033	2.025	2.000	2.000	2.000	2.000	2.000	2.000	2.046	2.033
Al	0.024		0.035	0.041	0.018	0.027	0.048						0.070	0.058	0.026	0.050	0.024	0.039	0.023	0.029	0.020	0.024
Ti	0.033	0.018	0.014	0.016	0.015	0.020	0.033	0.019	0.019	0.020	0.018	0.030	0.093	0.009	0.014	0.013	0.013	0.016	0.011	0.011	0.007	0.043
Fe^{3+}	0.169	0.053	0.411	0.247	0.155	0.114	0.449	0.033	0.016	0.076	0.058	0.060	0.472	0.203	0.047	0.091	0.087	0.198	0.154	0.109	0.396	0.484
Cr	0.000	0.001	0.001	0.000				0.003	0.001			0.001	0.002	0.000		0.000		0.000				
Zr	0.002		0.013	0.004	0.001	0.003	0.001	0.013		0.001	0.001	0.000	0.006	0.002	0.000	0.000		0.002	0.000	0.001	0.003	0.003
Mg	0.563	0.749	0.114	0.399	0.568	0.629	0.243	0.861	0.893	0.765	0.764	0.730	0.037	0.397	0.714	0.602	0.486	0.385	0.444	0.477	0.231	0.068
Fe^{2+}	0.208	0.179	0.410	0.292	0.243	0.207	0.226	0.072	0.071	0.138	0.159	0.178	0.321	0.331	0.199	0.245	0.390	0.357	0.368	0.373	0.335	0.377
Mn			0.002										0.000					0.002			0.008	
Sum M1	1.000	1.000	1.000	1.000	1.000	1.000	1.000	1.000	1.000	1.000	1.000	1.000	1.000	1.000	1.000	1.000	1.000	1.000	1.000	1.000	1.000	1.000
Mg																						
Fe^{2+}		0.017	0.000	0.025	0.018	0.043	0.024	0.013	0.032	0.006	0.028	0.007	0.051	0.024	0.034	0.022	0.010		0.005	0.003		0.028
Mn	0.015	0.006	0.020	0.014	0.013	0.008	0.013	0.002	0.003	0.010	0.009	0.006	0.006	0.012	0.008	0.015	0.018	0.016	0.023	0.023	0.013	0.011
Ca	0.912	0.937	0.358	0.598	0.779	0.787	0.286	0.984	0.948	0.942	0.925	0.957	0.099	0.608	0.897	0.868	0.868	0.854	0.816	0.855	0.409	0.249
Na	0.075	0.040	0.587	0.354	0.190	0.164	0.645	0.013	0.017	0.043	0.037	0.030	0.816	0.321	0.062	0.094	0.105	0.132	0.156	0.120	0.535	0.681
Sum M2	1.002	1.000	0.965	0.990	1.001	1.002	0.968	1.013	1.000	1.001	1.000	0.999	0.971	0.965	1.000	0.999	1.000	1.002	1.000	1.001	0.957	0.970
Sum Cat	4.002	4.000	4.013	4.004	4.001	4.002	4.000	4.013	4.000	4.001	4.000	3.999	4.004	3.991	4.000	3.999	4.000	4.002	4.000	4.001	4.003	4.003
End-members																						
Jd	1.3		2.6	2.5	1.0	1.5	3.7						6.6	3.5	1.3	2.7	1.3	2.2	1.3	1.5	1.4	2.0
Ae	2.9	2.1	40.8	19.4	9.6	7.6	46.3	0.7	0.9	2.2	2.0	1.6	70.9	16.9	1.9	2.5	4.3	5.3	7.4	4.9	36.5	52.9
Wo	42.9	46.9	25.5	36.0	42.6	42.3	19.7	47.8	47.3	45.7	46.0	46.5	0.5	36.7	45.6	43.9	45.2	42.0	43.3	44.6	28.5	16.6
En	31.7	38.8	8.4	24.7	31.7	34.7	18.9	44.2	45.5	40.2	39.7	38.3	3.5	24.3	37.3	32.6	25.9	22.0	24.5	25.8	16.4	5.5
Fs	12.6	10.4	21.6	16.3	14.3	12.9	8.9	4.5	5.4	8.1	10.2	10.0	9.7	18.0	12.6	15.3	22.2	21.5	21.8	21.5	16.7	19.6
Others	8.5	1.7	1.0	1.0	0.8	1.1	2.5	2.8	1.0	3.7	2.1	3.6	8.8	0.5	1.3	3.1	1.0	7.0	1.8	1.6	0.5	3.4

Table 3
Representative analyses of alkali feldspars from the Cerro Sarambí complex.

	Cerro Sarambí																Cerro Jhú		Cerro Teyú		Cerro Chiriguelo	
	Plutonic rocks								Dikes						Satellite plugs							
Sample	P41	P49	P49	P46	P39	P68	P68	P43	P37	P52	P56	P61	P61	P45	P34	P4	P10	P10	P17	P17	P28	P30
Rock type	mnsy	sd	sd	sy	sy	nsy	nsy	fen	min	trph	pht	pht	pht	ph	tr	tr	trph	trph	trph	trph	fen	fen
SiO_2	63.00	65.75	65.58	64.49	64.84	65.01	65.00	64.87	63.90	65.49	62.17	64.10	63.51	64.28	66.08	66.44	63.69	60.56	64.10	63.88	64.37	64.79
TiO_2		0.05	0.01	0.02			0.03	0.02	0.03	0.05	0.03	0.08	0.01	0.03	0.02	0.01	0.04	0.03	0.08	0.03		0.01
Al_2O_3	19.43	18.35	18.22	18.28	18.30	18.05	18.14	18.42	18.82	18.17	18.80	18.37	18.49	18.01	18.52	18.42	18.84	19.29	18.81	18.45	18.12	17.86
Fe_2O_3	0.10	0.49	0.60	0.47	0.37	0.92	0.95	0.46	0.29	0.54	0.55	1.16	0.26	0.68	0.56	0.62	0.33	0.97	0.18	0.66	0.63	0.81
MnO			0.01				0.02		0.01	0.01	0.01	0.02	0.01	0.04	0.02	0.01	0.01			0.03	0.01	
MgO	0.01		0.01					0.01		0.03	0.01	0.09	0.02	0.01	0.03		0.01	0.02	0.02		0.01	
BaO	0.82	0.23	0.03	0.10	0.11	0.43	0.35	0.42	1.17	0.15	2.14	0.21	1.19	0.46		0.12	1.69	5.28	0.82	0.45	0.62	0.07
CaO	0.14														0.48	0.17				0.01		
Na_2O	2.92	3.22	3.40	2.11	2.55	2.50	1.77	2.08	2.74	3.77	0.73	0.51	0.56	1.38	7.31	6.54	1.66	1.21	1.32	1.91	0.66	0.35
K_2O	12.04	12.39	12.41	14.27	13.59	13.35	14.33	14.42	12.56	11.89	14.66	16.17	15.62	15.16	5.87	7.59	14.43	13.39	14.96	14.00	16.33	16.83
SrO	1.24	0.20	0.23	0.02	0.19	0.34	0.32	0.05	0.50	0.11	1.09		0.09	0.22	0.16	0.10	0.23	0.29	0.29	0.39	0.05	
Total	99.70	100.68	100.50	99.76	99.95	100.60	100.91	100.75	100.02	100.21	100.19	100.71	99.76	100.27	99.05	100.02	100.93	101.04	100.58	99.81	100.80	100.72
Structural formulas calculated on the basis of 32 oxygens																						
Si	11.708	11.968	11.961	11.924	11.942	11.937	11.927	11.911	11.828	11.961	11.716	11.846	11.879	11.919	11.942	11.968	11.797	11.511	11.848	11.857	11.917	11.971
Al	4.253	3.933	3.913	3.981	3.969	3.903	3.920	3.983	4.103	3.908	4.172	3.998	4.073	3.933	3.942	3.908	4.110	4.318	4.094	4.033	3.951	3.886
Fe^{3+}	0.014	0.067	0.082	0.065	0.051	0.127	0.131	0.063	0.040	0.074	0.078	0.161	0.037	0.095	0.076	0.084	0.046	0.139	0.025	0.092	0.088	0.113
Ti		0.007	0.001	0.003			0.004	0.003	0.004	0.007	0.004	0.011	0.001	0.004	0.003	0.001	0.006	0.004	0.011	0.004		0.001
Mn			0.002				0.003		0.002	0.002	0.002	0.003	0.002	0.006	0.003	0.002	0.002			0.005	0.002	
Mg	0.003		0.003					0.003		0.008	0.003	0.025	0.006	0.003	0.008		0.003	0.006	0.006		0.003	
Ba	0.060	0.016	0.002	0.007	0.008	0.031	0.025	0.030	0.085	0.011	0.158	0.015	0.087	0.033		0.008	0.123	0.393	0.059	0.033	0.045	0.005
Sr	0.130	0.020	0.020		0.020	0.040	0.030	0.010	0.050	0.010	0.120		0.010	0.020	0.020	0.010	0.020	0.030	0.030	0.040	0.010	
Ca	0.028														0.093	0.033				0.002		
Na	1.052	1.136	1.202	0.756	0.911	0.890	0.630	0.741	0.983	1.335	0.267	0.183	0.203	0.496	2.562	2.284	0.596	0.446	0.473	0.687	0.237	0.125
K	2.855	2.877	2.888	3.366	3.193	3.127	3.355	3.378	2.966	2.770	3.525	3.812	3.727	3.586	1.353	1.744	3.410	3.247	3.528	3.315	3.857	3.967
Molecular components																						
Ab	26.7	28.3	29.4	18.3	22.2	22.2	15.8	18.0	24.9	32.5	7.0	4.6	5.2	12.2	63.9	56.2	14.9	12.1	11.8	17.2	5.8	3.1
Na	0.7	0.0	0.0	0.0	0.0	0.0	0.0	0.0	0.0	0.0	0.0	0.0	0.0	0.0	2.3	0.8	0.0	0.0	0.0	0.0	0.0	0.0
Or	72.6	71.7	70.6	81.7	77.8	77.8	84.2	82.0	75.1	67.5	93.0	95.4	94.8	87.8	33.8	42.9	85.1	87.9	88.2	82.8	94.2	96.9

Table 4
Representative analyses of micas from the Cerro Sarambí complex. Deficiencies of Si and ^{IV}Al on the tetrahedral site are filled completely by $^{IV}Fe^{3+}$ ($^{IV}Fe^{3+} = 8 - Si^{4+} - {}^{IV}Al^{3+}$), with the remaining $^{VI}Fe^{2+}$ ($^{VI}Fe^{2+} = Fe_{Tot} - {}^{IV}Fe^{3+}$) entering into the octahedral site.

	Cerro Sarambí																			
	Plutonic rocks			Dikes												Satellite plugs				
Sample	P49	P49	P49	P37	P37	P37	P56	P61	P61	P61	P52	P52	P52	P45	P45	P34	P34	P4	P4	P4
Rock type	sd	sd	sd	min	min	min	pht	pht	pht	pht	trph	trph	trph	ph	ph	tr	tr	tr	tr	tr
SiO_2	38.89	39.36	39.79	36.98	36.74	36.73	35.13	37.23	36.75	36.68	38.41	37.49	37.89	37.17	37.07	35.74	37.46	36.31	36.47	36.32
TiO_2	2.77	2.70	2.11	3.76	4.00	3.94	5.10	4.84	5.20	5.13	2.29	2.30	2.45	2.41	2.23	5.17	4.77	4.79	4.81	4.00
Al_2O_3	10.96	11.30	11.07	12.10	12.24	12.24	13.45	12.86	12.93	12.76	11.17	11.05	11.05	11.09	11.65	15.16	13.59	14.15	14.25	14.01
FeO	15.32	15.00	13.09	19.11	19.16	18.49	15.43	14.52	14.43	14.58	18.61	19.23	18.03	19.81	20.24	15.16	15.00	13.60	13.92	13.63
MnO	0.38	0.45	0.35	0.28	0.27	0.22	0.15	0.14	0.10	0.13	0.94	0.78	0.67	0.62	0.56	0.29	0.27	0.37	0.40	0.42
MgO	16.26	16.12	17.94	13.02	12.75	12.85	14.28	16.20	15.54	15.49	13.91	13.19	13.96	13.30	12.86	13.83	14.18	14.81	14.83	14.99
CaO	0.03		0.03				0.04	0.05	0.04			0.01	0.02	0.05	0.09		0.03			0.02
BaO	0.09	0.18	0.07	0.27	0.36	0.65	2.55	0.92	0.85	1.00	0.15	0.07	0.13	0.19	0.15	0.74	0.11	0.57	0.73	1.09
Na_2O	0.30	0.28	0.23	0.32	0.35	0.45	0.31	0.31	0.29	0.27	0.28	0.27	0.36	0.19	0.18	0.59	0.67	0.71	0.66	0.83
K_2O	9.89	10.02	10.13	9.74	9.62	9.69	8.67	9.37	9.48	9.60	10.03	9.66	9.80	9.60	9.65	8.92	9.17	9.15	9.17	8.92
F	1.50	1.22	1.60	0.99	0.98	0.82	0.06	0.01	0.14	0.25	1.45	2.51	2.10	1.05	1.02	1.39	0.98	2.89	3.42	2.98
Cl	0.02		0.03			0.01	0.01	0.02			0.01		0.02	0.01		0.03	0.02	0.01	0.01	0.02
Total	96.41	96.63	96.44	96.57	96.47	96.09	95.18	96.47	95.75	95.89	97.25	96.56	96.48	95.49	95.70	97.02	96.25	97.36	98.67	97.23
O-F-Cl	0.64	0.51	0.68	0.42	0.41	0.35	0.03	0.01	0.06	0.11	0.61	1.06	0.89	0.44	0.43	0.59	0.42	1.22	1.44	1.26
Ctotal	95.77	96.12	95.76	96.15	96.06	95.74	95.15	96.46	95.69	95.78	96.64	95.50	95.59	95.05	95.27	96.43	95.83	96.14	97.23	95.97
Structural formulas calculated on the basis of 11 oxygens																				
Si	2.992	2.996	3.029	2.871	2.857	2.857	2.706	2.775	2.769	2.775	2.985	3.013	3.003	2.936	2.922	2.731	2.841	2.837	2.849	2.859
Al^{IV}	0.994	1.004	0.971	1.107	1.122	1.122	1.221	1.130	1.148	1.138	1.015	0.987	0.997	1.033	1.078	1.269	1.159	1.163	1.151	1.141
Fe^{3+}	0.014			0.022	0.021	0.020	0.073	0.094	0.082	0.088				0.031						
Sum T	4.000	4.000	4.000	4.000	4.000	3.999	4.000	3.999	3.999	4.001	4.000	4.000	4.000	4.000	4.000	4.000	4.000	4.000	4.000	4.000
Al^{VI}		0.010	0.022								0.008	0.060	0.035		0.005	0.097	0.056	0.140	0.161	0.159
Ti	0.160	0.155	0.121	0.220	0.234	0.231	0.295	0.271	0.295	0.292	0.134	0.139	0.146	0.143	0.132	0.297	0.272	0.282	0.283	0.237
Fe^{2+}	0.972	0.955	0.833	1.219	1.225	1.183	0.921	0.811	0.827	0.835	1.210	1.292	1.195	1.277	1.334	0.969	0.951	0.889	0.909	0.897
Mn	0.025	0.029	0.023	0.018	0.018	0.014	0.010	0.009	0.006	0.008	0.062	0.053	0.045	0.041	0.037	0.019	0.017	0.024	0.026	0.028
Mg	1.865	1.829	2.036	1.507	1.478	1.490	1.640	1.800	1.746	1.747	1.612	1.580	1.649	1.566	1.511	1.576	1.603	1.725	1.727	1.759
Sum Oct.	3.022	2.968	3.013	2.964	2.955	2.918	2.866	2.891	2.874	2.882	3.018	3.064	3.035	3.027	3.014	2.861	2.843	2.920	2.945	2.921
Ca	0.002		0.002				0.003	0.004	0.003			0.001	0.002	0.004	0.008		0.002			0.002
Ba	0.003	0.005	0.002	0.008	0.011	0.020	0.077	0.027	0.025	0.030	0.005	0.002	0.004	0.006	0.005	0.022	0.003	0.017	0.022	0.034
Na	0.045	0.041	0.034	0.048	0.053	0.068	0.046	0.045	0.042	0.040	0.042	0.042	0.055	0.029	0.028	0.087	0.099	0.108	0.100	0.127
K	0.971	0.973	0.984	0.965	0.954	0.962	0.852	0.891	0.911	0.926	0.994	0.990	0.991	0.967	0.970	0.870	0.887	0.912	0.914	0.896
Sum Interl.	1.021	1.019	1.022	1.021	1.018	1.050	0.978	0.967	0.981	0.996	1.041	1.035	1.052	1.006	1.011	0.979	0.991	1.037	1.036	1.059
CF	0.365	0.294	0.385	0.243	0.241	0.202	0.015	0.002	0.033	0.060	0.356	0.638	0.526	0.262	0.254	0.336	0.235	0.714	0.845	0.742
CCl	0.003		0.004			0.001	0.001	0.003			0.001		0.003	0.001		0.004	0.003	0.001	0.001	0.003
OH	1.632	1.706	1.611	1.757	1.759	1.797	1.984	1.995	1.967	1.940	1.642	1.362	1.471	1.736	1.746	1.660	1.762	1.285	1.154	1.256

earth elements; noble gases (Ar, Xe, Kr, Ne and He); and stable and radiogenic isotopes.

Cerro Guazú, 70 km SSW of the city of Pedro Juan Caballero, is geologically poorly known and referred to as an oval stock of shonkinite, a coarse and fine-grained mela-syenite that shows evidence of fenitization, surrounded by strongly silicified sandstones and conglomerates of the Triassic-Jurassic Misiones Formation. Carbonatite is presumed to occur at depth due to geophysical data and geochemical anomalies for REE, Nb, Sr, and Ba (Mariano and Druecker, 1985). Large boulders of partially weathered lamprophyres found on the surface of the northwest slopes of Cerro Guazú are described by Mariano (1978). A radial dike swarm of lamprophyres and trachyte porphyries is also reported.

Not much information does exist in Paraguayan literature for the small intrusions of Arroyo Gasory and Cerro Tayay. Mariano (1978) mentions the occurrence of a dike of trachyte porphyry at Arroyo Gasory, about 15 km WSW of the Cerro Chiriguelo complex. Cerro Tayay has been reported by Livieres and Quade (1987) as a morphological feature conical in shape, with a radial structure and presence of ultramafic(?) rocks. A brief reference is made by Wiens (1991) to a residual aeromagnetometric positive anomaly at the southern portion of Cerro Tayay, probably indicating a volcanic structure, and to the occurrence of flood basalts occupying the high parts of the hill. The author also calls attention to aeromagnetometric and radiometric anomalies over the whole area, which could represent alkaline bodies, such as Cerro Jhú and Cerro Teyú. In fact, trachyphonolites and analcime phonolites form an impressive plug in Cerro Jhú, while partially altered trachyphonolites intruded into Early Cretaceous sedimentary deposits are found in Cerro Teyú (also referred to as Colônia Indígena Itaipausú by Paula, 2004) probably as dikes in association with reddish sandstones.

4. Petrographic features

Field work in December 2003 in the Amambay area, generally difficult to access due to security issues and private interests, allowed rocks from the Cerro Sarambí and a few samples from the nearby intrusions of Cerro Apuá, Cerro Chiriguelo, Cerro Jhú and Cerro Teyú to be collected. The investigated samples include rocks belonging to plutonic and volcanic suites, the latter consisting mostly of lithological types forming plugs and dikes. The plutonic suite is represented by SiO_2-undersaturated to saturated syenitic rocks, sometimes deeply influenced by fenitization processes, and by the Cerro Chiriguelo carbonatites. The volcanic suite comprises rocks of syenitic affinity (trachyte, trachyphonolite, phonolite) and mafic composition (tephrite, phonotephrite). The volcanic group of syenitic affinity is represented by dikes (trachyphonolite, phonolite) and satellite plugs (trachyte) associated with the Cerro Sarambí complex and the trachyphonolite occurrences of Cerro Jhú and Cerro Teyú. The more mafic rock types, tephrite and phonotephrite, are found only as dikes in Cerro Sarambí.

Accounting only for the Cerro Sarambí silicate rocks, the plutonic types are represented by syenites, nepheline syenites, syenodiorites, and mela-nepheline syenites. The rocks are generally massive, medium to coarse-grained, alotriomorphic to porphyritic, and contain large alkali feldspar laths in addition to clinopyroxene, sometimes forming clustered aggregates that appear as black masses in hand specimens. Generally, alkali feldspar and clinopyroxene are the most abundant minerals and, consequently, the more important felsic and mafic phases, respectively, of these rocks. Other minerals include nepheline, biotite, amphibole, and occasionally melanite. Apatite, titanite, opaques, and zircon are frequent accessory phases, while alteration minerals consist principally of carbonates and zeolites. In many cases, the nepheline syenites and the mela-nepheline syenites exhibit clear evidence of fenitization, a metasomatic process responsible for the formation of granular to oriented rocks having elongated sodic clinopyroxene (aegirine) prisms and alkali feldspar laths.

Table 5
Representative analyses of nepheline from the Cerro Sarambí complex.

	Cerro Sarambí		
	Plutonic rocks		
Sample	P41	P41	P41
Rock type	mnsy	mnsy	mnsy
SiO_2	44.04	44.00	44.18
TiO_2	0.04		0.02
Al_2O_3	33.21	32.87	32.88
Fe_2O_3	0.60	0.63	0.55
MnO			0.01
CaO	0.10	0.07	0.08
Na_2O	16.51	16.72	16.54
K_2O	6.20	6.16	6.03
Total	100.70	100.45	100.29
Structural formulas calculated to 32 oxygens			
Si	8.408	8.428	8.457
Al	7.466	7.415	7.412
Ti	0.006		0.003
Fe^{3+}	0.086	0.091	0.079
Mn			0.002
Na	6.111	6.210	6.139
Ca	0.020	0.014	0.016
K	1.510	1.505	1.473
Molecular components			
Q	8.88	8.13	9.61
Ne	72.68	73.68	72.59
Ks	17.96	17.86	17.42
An	0.48	0.33	0.38
Mg, Ba, Sr – below detection limits			

The volcanic suite exhibits aphyric to porphyritic texture and alkali feldspar, and feldspathoids (nepheline, analcime), clinopyroxene, and biotite as main phenocrysts to microphenocrysts set in a groundmass formed basically of the same minerals. Trachytic-type texture is typical of rocks displaying an accentuated subparallel orientation of alkali feldspar microlites. The mafic-ultramafic rocks are characteristically porphyritic in texture with the phenocrysts to microphenocrysts represented mostly by mafic minerals (clinopyroxene, olivine, biotite), plagioclase, and feldspathoids. They are usually set in a hyaline to hypocrystalline groundmass with alkali feldspar, clinopyroxene, olivine, biotite, feldspathoids (nepheline, analcime), and opaques. Accessory minerals are apatite and zircon.

The only description available for the Cerro Sarambí carbonatites is that from Castorina et al. (1996) with the rocks represented by calciocarbonatite veins and medium-grained silicocalciocarbonatite stringers bearing fluorite, vermiculite, and opaques as accessories.

5. Analytical procedures

Samples of the Amambay Province, mostly from the Cerro Sarambí complex, were analyzed for major, trace, and rare earth elements using ICP-OES (inductively coupled plasma-optical emission spectrometry) and ICP-MS (inductively coupled plasma-optical spectrometry) methods at the Actlabs in Canada. Sr and Nd isotope analysis were performed at the Geochronological Research Center of the Institute of Geosciences of the University of São Paulo (IGc-USP) with a VG 354 Micromass multicollector mass spectrometer following the procedures described in Sato et al. (1995). Mineral compositions were determined utilizing a Jeol JXA-8600 electron

microprobe, which was equipped with five wavelengths dispersive spectrometers (WDS), at the IGc. Operating conditions were accelerating voltage of 15 kV and a probe current of 20 nA. Peak counting times ranged from 5–20″ for major elements to 40″ for minor and trace elements. Silicate minerals and synthetic oxides were employed as standards and the data were corrected on-line using the PROZA procedure (Bastin and Heiligers, 1990).

6. Mineral chemistry

Chemical analyses for the most widespread minerals of the alkaline rocks from the Amambay area are provided in Tables 2–6. Not shown are the accessory Fe–Ti oxides, represented mostly by an almost pure magnetite with more than 0.99 of $Fe^{2+}/(Fe^{2+}+Mg)$, very low Al (<0.7 a.f.u.) and Mg (<0.6 a.f.u.), and in some nepheline syenites and phonotephrites from Cerro Sarambí, containing Ti up to 2.3 a.f.u.

Clinopyroxenes are the main mafic constituent of the Cerro Sarambí rocks. Following Morimoto's (1988) classification, the mineral belongs to the diopside-hedenbergite-augite-(aegirine-augite)-aegirine series (Figs. 2A, Table 2). In the plutonic suite, clinopyroxenes from nepheline syenites, syenodiorites, and melanepheline syenites exhibit composition almost restricted to the diopside field ($Wo_{42-47}En_{31-41}Fs_{7-14}$), but in more evolved syenitic rocks they may reach the aegirine-augite field ($Ae_{18-19}Jd_{2-3}$). In the volcanic suite, clinopyroxenes from tephrite, tephriphonolite, and phonotephritic dikes and from trachyte plugs are represented by diopside ($Wo_{43-48}Mg_{32-46}Fe_{4-16}$) and aegirine-augite ($Ae_{16-22}Jd_{2-4}$) in phonolites. In the Cerro Jhú and Cerro Teyú occurrences, the composition corresponds to diopside-hedenbergite ($Wo_{42-45}Mg_{22-27}Fe_{21-23}$).

Fenite clinopyroxenes are aegirine-augite, displaying compositional enrichment in $^{VI}Fe^{3+}$ (0.406–0.551 a.f.u) and Na (0.515–0.712 a.f.u), a typical feature of potassic fenites associated with carbonatites (Le Bas, 2008). The most evolved compositions (aegirine, $Ae_{56-73}Jd_{3-6}$, and aegirine-augite, $Ae_{16-38}Jd_{2-3}$) are found in the phonotephritic dike P61 and syenite P46, respectively, both being related to fenitization processes.

The main evolutionary trend of the Cerro Sarambí clinopyroxenes is characterized by the progressive enrichment in Fe^{3+} and Na, a pattern common to several Brazilian alkaline rocks. Fig. 2B shows various lines of evolution for rock associations from different occurrences.

Alkali feldspars are the main felsic mineral of the Cerro Sarambí rocks. In both plutonic and dike suites, the composition is almost similar, varying in the interval $An_{0-1}Ab_{5-32}Or_{67-95}$ (Fig. 3, Table 3). Cerro Teyú and Cerro Jhú occurrences have values in the same range $An_0Ab_{5-17}Or_{83-95}$. The satellite trachytic plugs differ in that they contain alkali feldspars more enriched in the Ab component ($An_{1-3}Ab_{42-64}Or_{34-56}$); the fenites exhibit small

Table 6
Representative analyses of garnets from the Cerro Sarambí complex. Structural formulas and end-members calculated according to Locock (2008).

	Cerro Sarambí					Cerro Jhú		Cerro Chiriguelo			
	Plutonic rocks			Dikes							
Sample	P46	P46	P46	P45	P45	P10	P10	P28	P28	P28	P28
Rock type	sy	sy	sy	ph	ph	trph	trph	fen	fen	fen	fen
SiO_2	34.11	33.09	34.39	32.96	32.2	31.41	31.88	31.99	32.25	32.47	33.82
TiO_2	3.05	2.95	1.86	5.97	5.53	8.43	7.72	8.01	7.03	6.18	4.08
Al_2O_3	0.81	0.61	0.96	1.14	0.28	1.57	1.55	0.39	0.39	0.29	0.27
Cr_2O_3	0.01							0.03			0.01
FeO_{tot}	25.4	24.4	24.45	23.09	23.74	21.83	21.97	23.18	23.88	24.15	24.45
MnO	0.41	0.41	0.35	0.44	0.38	0.39	0.41	0.37	0.29	0.36	0.78
MgO	0.17	0.22	0.15	0.23	0.22	0.37	0.33	0.25	0.23	0.21	0.09
CaO	31.85	32.03	32.58	30.72	32.09	32.19	32.4	32.21	32	32.01	31.99
Na_2O	0.16	0.31	0.13	0.34	0.26	0.16	0.14	0.37	0.31	0.29	0.28
Total	95.97	94.02	94.87	94.89	94.7	96.35	96.4	96.8	96.38	95.96	95.77
Structural formulas calculated to 8 cations and 12 anions											
Si	2.914	2.876	2.957	2.854	2.798	2.686	2.721	2.728	2.761	2.789	2.901
Al	0.082	0.062	0.043	0.116	0.029	0.158	0.156	0.039	0.039	0.029	0.027
Fe^{3+}	0.004	0.061		0.030	0.174	0.155	0.123	0.232	0.200	0.182	0.072
Sum T	3.000	3.000	3.000	3.000	3.000	3.000	3.000	3.000	3.000	3.000	3.000
Ti	0.196	0.193	0.120	0.389	0.361	0.542	0.496	0.514	0.453	0.399	0.263
Al			0.054								
Cr	0.001							0.002			0.001
Fe^{2+}	0.083			0.186	0.028	0.150	0.136	0.118	0.125	0.093	0.063
Fe^{3+}	1.720	1.713	1.758	1.425	1.523	1.255	1.310	1.303	1.385	1.461	1.619
Mn^{3+}		0.030	0.012								
Mg		0.029	0.019		0.028	0.047	0.042	0.032	0.029	0.027	0.012
Sum Oct.	2.000	1.964	1.964	2.000	1.941	1.995	1.984	1.969	1.992	1.980	1.957
Fe^{2+}	0.007			0.031							
Mn^{2+}	0.030		0.013	0.032	0.028	0.028	0.030	0.027	0.021	0.026	0.057
Mg	0.022			0.030							
Ca	2.915	2.983	3.001	2.850	2.987	2.950	2.963	2.943	2.935	2.946	2.940
Na	0.027	0.052	0.022	0.057	0.044	0.027	0.023	0.061	0.051	0.048	0.047
Sum Dodc.	3.000	3.036	3.036	3.000	3.059	3.005	3.016	3.031	3.008	3.020	3.043
End-members											
Andradite	84	86	88	68	76	62	66	65	69	73	81
Schorlomite	4	6	2	7	10	16	14	14	12	10	5
Morimotoite	8	2	2	19	6	20	18	15	16	12	7
Grossular			3								
Others	4	6	5	6	8	2	2	6	3	5	7

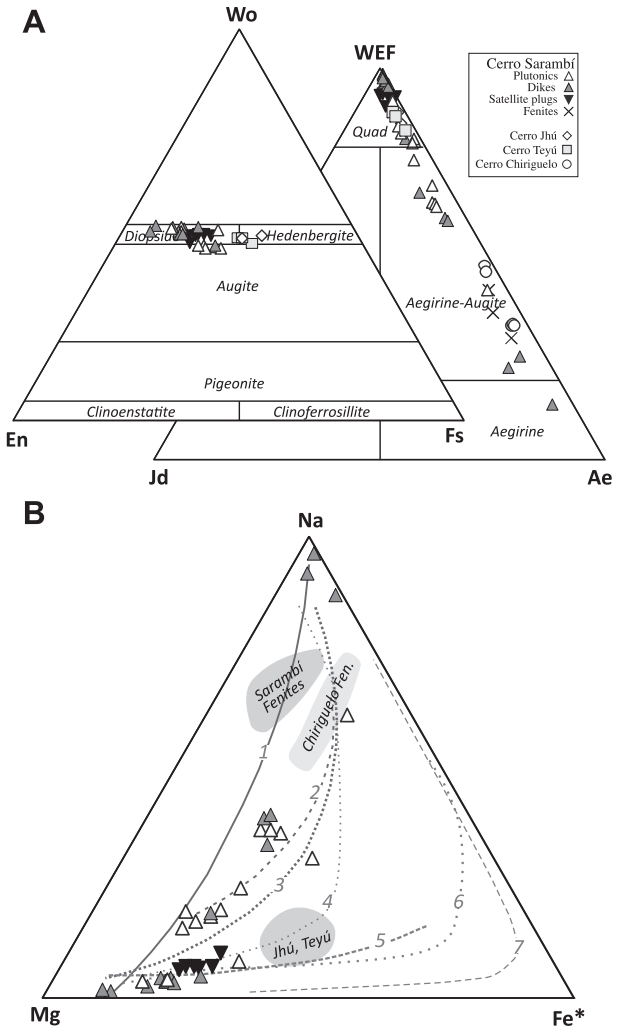

Fig. 2. A) Classification of Cerro Sarambí clinopyroxenes according to Morimoto (1988). B) Compositional fields for some Amambay occurrences are plotted on the Na–Mg–Fe* ($Fe^* = Fe^{2+} + Fe^{3+} + Mn - Na$) diagram. Main trend lines for clinopyroxenes of Brazilian alkaline rocks are shown for comparison: 1, Anitápolis (Furtado and Gomes, 1994); 2, Itapirapuã (Gomes et al., 1970); 3, Banhadão (Ruberti, 1984); 4, Passa Quatro (Brotzu et al., 1992); 5, Morro Redondo (Brotzu et al., 1989); 6, Monte de Trigo Island (Enrich, 2005); 7, Cananeia (Spinelli and Gomes, 2009).

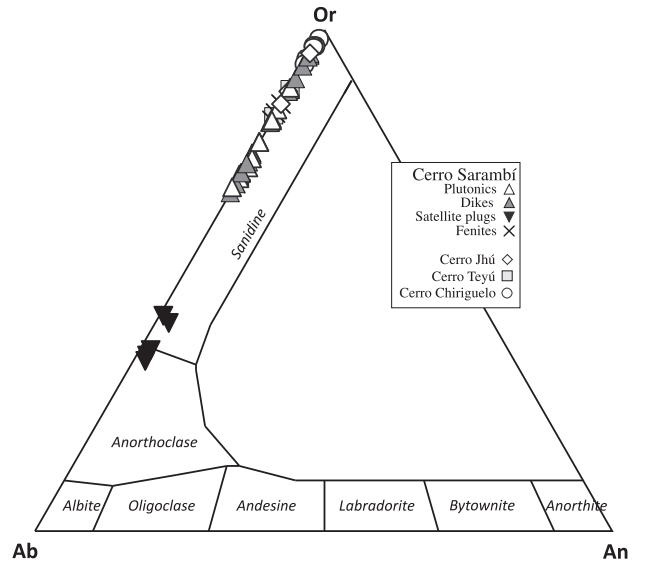

Fig. 3. Compositional variation of alkali feldspars from the Cerro Sarambí complex in the An–Ab–Or diagram.

variations in composition, as the Cerro Sarambí minerals are more sodic in relation to those of the Cerro Chiriguelo ($An_0Ab_{14-18}Or_{82-85}$ and $An_{0-1}Ab_{1-7}Or_{93-98}$, respectively). These values are in total agreement with the worldwide compositions shown by potassic fenites developed around calcite-rich carbonatites (Le Bas, 2008).

Micas are the only H_2O-bearing mafic minerals identified in rocks of the Cerro Sarambí area, being particularly abundant in the ultramafic-mafic dikes. All the compositions belong to the phlogopite-annite series (Fig. 4A, Table 4). Small deficiencies in the tetrahedral site (i.e. $Si + Al < 8$) have been completed with Fe^{3+}, the remaining iron assumed to be Fe^{2+} and used for filling the octahedral site, a procedure adopted by various authors (e.g., Shaw and Penczak, 1996; Brod et al., 2001; Brigatti and Guggenheim, 2002). The ^{IV}Al-deficiency is interpreted as a direct consequence of the peralkalinity of the magma (Mitchell and Bergman, 1991; Mitchell, 1995). However, biotites from the trachytic satellite plugs show excess Al, reaching at least 0.140 (a.f.u.) in the octahedral site (Al^{VI}) of the Cerro Apuá occurrence.

The Cerro Sarambí biotites contain considerable concentrations of Ti, with TiO_2 ranging from 2.1 to 5.2 wt% (Table 4). The phonotephrite and tephrite dikes and the trachytic plugs display the highest concentrations. The Ti^{4+} allocation to the octahedral site involves Ti-Tschermak ($^{VI}R^{2+} + 2 * {}^{IV}Si^{4+} = {}^{VI}Ti^{4+} + 2 * {}^{IV}Al^{3+}$), Ti-vacancy ($2 * {}^{VI}R^{2+} = {}^{VI}Ti^{4+} + {}^{VI}\square$), and Ti-oxy ($^{VI}R^{2+} + 2 * (OH)^- = {}^{VI}Ti^{4+} + 2 * O^{2-} + H_2$) coupled substitutions to balance the charge differences (Mansker et al., 1979; Zhang et al., 1993; Henderson and Foland, 1996; Laurora et al., 2007). For the Cerro Sarambí phlogopite-biotites, both Ti-Tschermak- and Ti-vacancy coupled substitutions are the key operative mechanisms (Fig. 4B and C), as also concluded by Azzone et al. (2009) for the Ti-rich biotites from the Ponte Nova massif. The Ti-oxy substitution cannot be tested because of the unknown H_2O content of the micas, although the low totals suggest that this mechanism may not be relevant.

Nepheline constitutes the most important mineral of the feldspathoid group, being altered to cancrinite in most cases. Representative compositions of fresh nephelines are found in the mela-nepheline syenites (Table 5), with the mineral showing compositional range $Ne_{72-74}Q_{8-10}Ks_{17-18}$ close to the Morozewicz composition (Fig. 5; Tilley, 1954) and equilibrium temperatures between 500 °C and 700 °C (Hamilton and McKenzie, 1960; Hamilton, 1961).

Garnet is a common accessory phase in syenites and phonolites from the Cerro Sarambí, in fenites from the Cerro Chiriguelo, and in trachyphonolites from the Cerro Jhú. It is represented by a calcic type showing TiO_2 content variable from 1.86 up to 8.43 wt% (Table 6). In general, crystals of the plutonic lithotypes are less enriched in Ti (0.120–0.196 a.f.u.) in relation to those of volcanic rocks and fenites (0.263–0.542 a.f.u.). On the whole, the mineral contains very low Al content (0.027–0.158 a.f.u). These garnets can be considered mainly as a solid solution of andradite ($Ca_3Fe^{3+}{}_2Si_3O_{12}$), morimotoite [$Ca_3Ti(Mg,Fe^{2+})Si_3O_{12}$], and schorlomite [$Ca_3Ti_2(Si,Fe^{3+},Al,Fe^{2+})_3O_{12}$] components, according to Locock (2008). Furthermore, the excess of Fe^{3+} compared to the Ti concentrations in the octahedral site allows the classification as melanite (Howie and Woolley, 1968).

Ti-rich garnets are also found in occurrences of nepheline syenites and phonolites from southeastern Brazil, such as Itapirapuã (Gomes et al., 1968), Banhadão (Ruberti, 1984), Itatiaia (Brotzu et al., 1997), and Morro de São João (Brotzu et al., 2007).

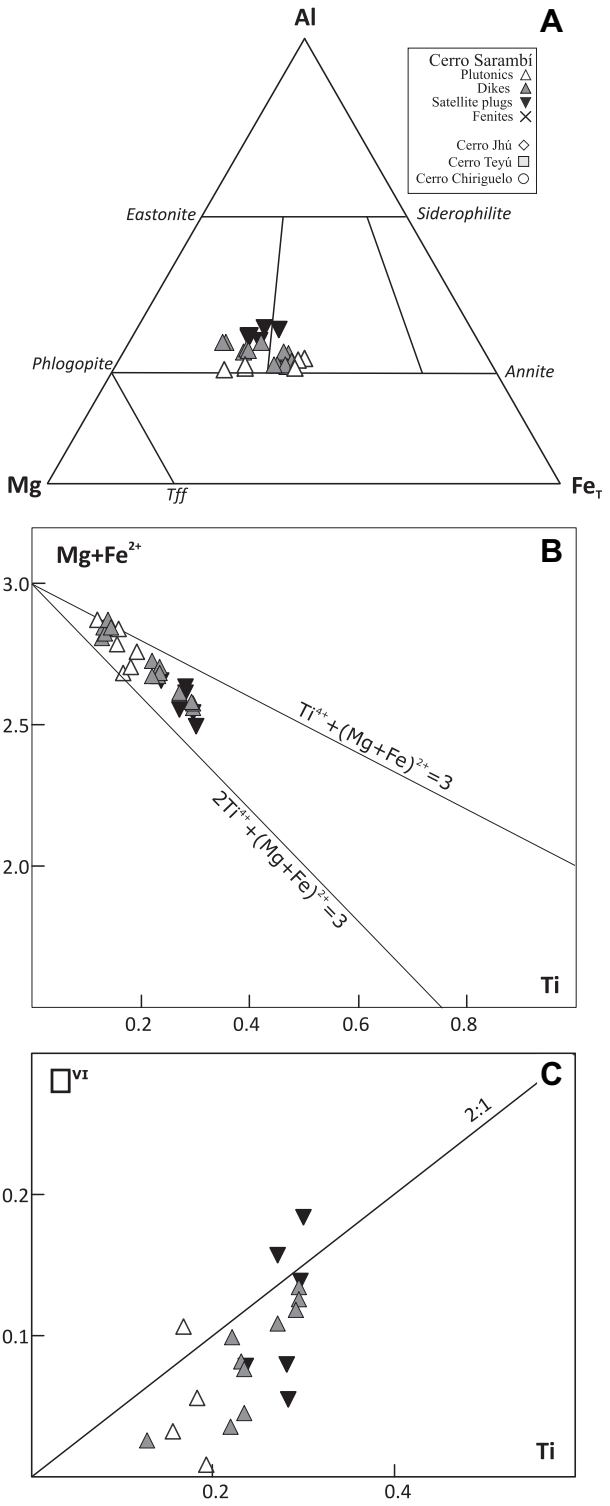

Fig. 4. A) Compositional variation of micas from the Cerro Sarambí complex in the Mg–Al–Fe$_{tot}$ diagram. B–C) Ti (a.f.u.) vs. Mg + Fe^{2+}(a.f.u.) and octahedral vacancies (a.f.u.), respectively.

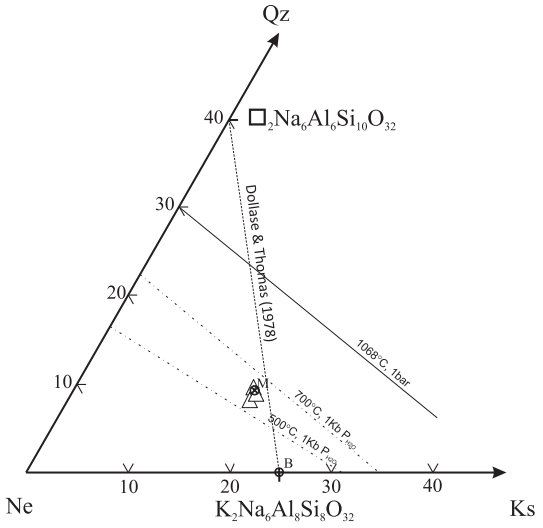

Fig. 5. Nepheline compositions for plutonic rocks from the Cerro Sarambí complex in the Qz–Ne–Ks molecular proportion diagram. Equilibrium temperatures according to Hamilton and McKenzie (1960) and Hamilton (1961). Also shown are references to the Morozewicz (M) and Buerger (B; Tilley, 1954) compositions and the compositional plane of Dollase and Thomas (1978).

7. Geochemistry

Table 7 lists 17 analyses of silicate alkaline rocks from the Amambay area (data after Paula, 2004). The analyses represent mostly Cerro Sarambí rocks (13); the remaining samples are associated with the occurrences of Cerro Chiriguelo (2), Cerro Jhú, and Cerro Teyú. Table 7 also shows two analyses of carbonatite from Cerro Chiriguelo.

On the K_2O vs. Na_2O diagram (Middlemost, 1975), the silicate rocks fall entirely into the potassic and highly potassic series (Fig. 6). When plotted into the De La Roche et al. (1980) classification diagram (Fig. 7), the plutonic types of the Cerro Sarambí complex are concentrated mainly in the SiO_2-undersaturated to saturated syenitic fields. Compositions of the dikes suggest an evolutionary trend from tephrite to phonotephrite, then to trachyphonolite and finally to phonolite. The satellite plugs show a trachyte composition. The Cerro Jhú and Cerro Teyú rocks are restricted to the trachyphonolite (nepheline syenite) field; the same applies to the Cerro Sarambí and Cerro Chiriguelo fenites. Agpaitic ratios for the entire set of silicate rocks range from 0.68 to 0.93, clearly indicating a miaskitic affinity (cf. Sørensen, 1960). Variation diagrams of major and trace elements against SiO_2 concentration for the Amambay silicate rocks are displayed in Figs. 8 and 9. In particular, regarding the Cerro Sarambí complex, positive correlations are indicated for Al_2O_3, K_2O, and Rb, but negative ones for TiO_2, Fe_2O_3, CaO, P_2O_5, and Co. Scattered values for Na_2O contents are due possibly to the action of fenitization processes. Although the Amambay rocks vary in abundance, they are rich in Sr and Ba, especially the Cerro Chiriguelo carbonatites.

Incompatible elements normalized to primitive mantle (McDonough and Sun, 1995) for both plutonic and volcanic rocks show positive anomalies for Rb, La, Pb, Sr, and Sm, an irregular behavior of K and Zr + Hf, and negative spikes for Nb–Ta, P, and Ti (Fig. 10). These last peaks are considerably more pronounced in the Cerro Sarambí and Cerro Chiriguelo carbonatites, as indicated in Fig. 10F. In particular, the behavior of incompatible and rare earth elements in both carbonatites is discussed more exhaustively by Castorina et al. (1996, 1997) and Comin-Chiaramonti et al. (2005, 2007b).

Chondrite-normalized rare earth elements patterns (McDonough and Sun, 1995) for both suites are characterized by high REE concentrations and strong LREE/HREE fractionation (Fig. 11). With the exception of one sample of reomorphic fenite from Cerro Chiriguelo (Fig. 11C), all the rocks yielded an almost parallel pattern. The positive correlation between REE and TiO_2 and P_2O_5 indicates that the crystallization of accessory phases such as titanite, melanite, and apatite have exerted some control on the behavior of the incompatible elements. In this way, the concave-

Table 7
Chemical analyses of alkaline rocks from the Amambay area. Also included are the R1 and R2 parameters (De La Roche et al., 1980) and the A.I. (agpaitic index, $Na_2O + K_2O/Al_2O_3$ molar, cf. Sørensen 1960) and mg# ($MgO/FeO + Fe_2O_3$) values. Fe contents are expressed as Fe_2O_3. Abbreviations: Cc, calciocarbonatite.

	Cerro Sarambí												
	Plutonic rocks						Dikes					Satellite plugs	
Sample	P41	P49	P46	P39	P68	P43	P37	P52	P56	P61	P45	P34	P4
Rock type (wt%)	mnsy	sd	sy	sy	nsy	fen	min	trph	pht	pht	ph	tr	tr
SiO_2	50.67	54.99	63.03	60.04	59.81	59.21	48.31	55.80	46.41	49.69	52.60	59.94	61.93
TiO_2	1.22	1.86	0.25	0.89	0.92	0.82	2.00	1.23	1.65	1.88	1.87	0.61	0.59
Al_2O_3	15.81	11.76	17.71	16.05	14.93	15.62	10.94	15.51	14.55	12.76	15.46	16.63	16.87
Fe_2O_3	7.52	8.73	1.56	4.88	6.21	6.44	10.04	7.05	9.04	9.50	10.01	3.89	3.83
MnO	0.14	0.15	0.03	0.09	0.14	0.13	0.15	0.15	0.16	0.14	0.14	0.08	0.08
MgO	2.61	3.06	0.27	1.02	0.99	0.61	6.96	1.58	3.03	1.55	1.40	0.62	0.77
CaO	7.41	6.24	1.00	2.78	2.11	2.57	9.64	4.27	7.35	7.28	4.21	2.66	2.09
Na_2O	4.87	2.74	1.77	3.44	4.74	3.81	3.25	4.64	2.96	3.08	4.31	5.25	5.46
K_2O	6.42	7.39	13.33	9.34	8.48	9.61	5.63	7.54	7.07	7.44	8.30	6.24	6.04
P_2O_5	0.62	0.76	0.12	0.20	0.20	0.16	0.81	0.48	0.66	0.73	0.29	0.18	0.18
LOI	1.39	1.10	0.88	0.70	1.38	1.26	1.25	1.33	7.07	6.27	0.94	2.81	1.40
Total	98.67	98.78	99.94	99.43	99.91	100.23	98.98	99.57	99.94	100.33	99.53	98.91	99.24
R_1	−74	697	409	450	140	163	446	99	120	192	−264	556	663
R_2	1232	1050	468	663	568	612	1591	840	1222	1106	823	642	593
A.I.	0.95	1.06	0.98	0.98	1.14	1.07	1.05	1.02	0.86	1.03	1.04	0.93	0.92
mg#	40.7	41.0	25.5	29.3	24.0	15.8	57.9	30.8	39.9	24.4	21.7	24.0	28.5
ppm													
Sc	8	17	1	6	4	3	25	9	11	14	5	4	6
V	124	200	56	105	115	123	236	138	197	203	236	59	65
Cr	41	54	23	41		40	113	27				36	57
Co	15	20	1	6	13	5	34	11	20	23	22	5	6
Ni						28	30						165
Cu	16	45	13					15	25	48	15	12	17
Zn	95	112		65	115	114	103	100	100	113	53	66	61
Ga	18	18	26	19	28	29	20	22	21	19	24	20	21
Rb	86	146	184	141	181	177	135	119	114	106	124	110	115
Sr	4153	2072	1889	2845	2342	2661	2682	3527	6185	1078	4058	2302	2265
Cs	1.3	1.5	0.8	0.6	2.5	2.3	2.0	1.1	7.5	1.4	1.1	1.3	1.0
Ba	3798	4856	3482	3128	2573	3382	3040	3043	3688	4413	5699	2845	2490
Y	22	32	6	21	26	11	25	28	22	37	10	19	19
Zr	454	323	147	214	1022	782	412	561	514	558	517	454	478
Hf	13.1	9.9	3.9	6.9	24.6	19.6	11.8	14.5	13.7	14.6	15.3	13.0	11.6
Nb	86	59	33	57	94	62	69	68	76	75	89	79	52
Sn	4	4	1	3	3	4	3	3	3	4	3	3	3
Ta	5.2	4.0	0.8	2.8	3.3	1.6	3.3	3.4	4.0	4.4	5.2	3.6	3.2
Tl	1.8	2.3	1.9	1.5	2.1	2.6	1.9	2.0	1.9	1.6	1.2	1.7	1.5
Pb	33	26	27	13	74	28	18	34	23	34	6	56	47
Th	18.3	19.8	8.3	6.9	61.2	26.1	21.2	20.9	23.3	24.3	14.2	29.5	30.0
U	3.7	3.9	2.1	1.0	11.4	3.6	5.5	3.9	5.1	3.7	1.2	6.6	6.6
La	205	194	57.8	126	180	172	177	183	205	198	254	154	150
Ce	389	379	101	239	286	266	335	328	379	377	418	267	241
Pr	42.3	42.4	9.81	24.8	26.4	23.8	37.5	33.9	40.5	42.1	39.9	26.8	23.4
Nd	140	144	30.5	80.1	79.9	67.2	129	110	134	144	116	83.8	71.6
Sm	19.5	21.5	4.1	11.6	10.9	8.0	19.0	16.0	18.9	21.9	13.0	11.5	9.8
Eu	5.09	5.13	1.02	2.86	2.85	1.83	4.51	4.07	4.97	5.76	2.89	2.94	2.49
Gd	10.2	12.5	2.3	6.8	6.3	3.8	10.7	9.7	10.4	13.3	6.1	6.4	5.5
Tb	1.1	1.5	0.3	0.9	0.9	0.5	1.2	1.1	1.1	1.6	0.6	0.8	0.7
Dy	5.2	7.1	1.3	4.4	4.7	2.5	5.6	5.8	5.2	7.6	2.6	3.8	3.5
Ho	0.8	1.1	0.2	0.8	0.9	0.4	0.9	1.0	0.8	1.3	0.4	0.6	0.6
Er	2.1	3.1	0.6	2.1	2.8	1.4	2.6	3.0	2.1	3.5	1.0	2.0	2.0
Tm	0.26	0.39	0.08	0.28	0.42	0.23	0.31	0.41	0.27	0.43	0.12	0.26	0.26
Yb	1.6	2.5	0.5	1.8	2.8	1.7	2.1	2.6	1.7	2.7	0.8	1.8	1.7
Lu	0.21	0.32	0.06	0.24	0.40	0.26	0.27	0.37	0.21	0.36	0.13	0.24	0.24

	Cerro Jhú	Cerro Teyú	Cerro Chiriguelo			
			Fenites		Carbonatites	
Sample	P11	P17	P28	P30	P24	P26
Rock type (wt%)	trph	trph	nsy	nsy	cc	cc
SiO_2	53.98	57.98	56.49	52.52	3.7	1.64
TiO_2	0.82	0.42	1.76	0.46	0.05	0.02
Al_2O_3	14.11	16.93	12.62	15.23	0.64	0.12
Fe_2O_3	7.45	4.43	9.17	11.86	3.23	1.68
MnO	0.22	0.14	0.19	0.14	0.32	0.11
MgO	1.37	0.31	0.24	0.41	1.47	0.2
CaO	5.72	2.03	5.60	2.42	42.98	51.26
Na_2O	3.44	5.01	0.88	6.50		

(*continued on next page*)

Table 7 (*continued*)

	Cerro Jhú	Cerro Teyú	Cerro Chiriguelo			
			Fenites		Carbonatites	
Sample	P11	P17	P28	P30	P24	P26
Rock type (wt%)	trph	trph	nsy	nsy	cc	cc
K_2O	7.79	9.36	10.87	7.04	0.71	
P_2O_5	0.32	0.07	0.13	0.01	0.35	0.78
LOI	3.65	2.72	0.93	1.95	35.32	40.18
TOTAL	98.87	99.40	98.88	98.54	88.76	95.95
R_1	346	−226	636	−764	−2	67
R_2	957	565	859	578	4684	5497
A.I.	1.00	1.09	1.05	1.20		
mg#	26.7	12.2	4.9	6.4		
ppm						
Sc	6	2	3			
V	240	111	493	293	39	90
Cr	29	58				
Co	6	2	14	4		
Ni	−20	72				48
Cu	11		11	17	29	36
Zn	136	109	188	61	97	31
Ga	17	24	22	27	12	3
Rb	126	160	114	88	55.0	6.0
Sr	3211	2083	731	2763	37527	3722
Cs	1.2	1.2	0.9	0.9	5.7	2.6
Ba	5826	4536	9140	847	18386	18720
Y	42	22	52	6	4.0	4.0
Zr	701	824	1050	2591	3	18.0
Hf	17.7	18.7	24.7	52.2	1.50	0.70
Nb	114	93	161	259	51.0	18.0
Sn	4	3	6	4		
Ta	3.5	1.8	5.7	11.2	0.20	
Tl	2.3	3.2	1.3	2.1	36.8	2.9
Pb	40	58	81	15	845	145
Th	42.4	47.6	26.9	19.0	4.00	6.40
U	9.7	11.4	7.9	3.5	9.40	5.20
La	312	146	197	322	484	478
Ce	473	237	279	435	660	662
Pr	50.9	21.6	44.9	30.4	60.5	59.0
Nd	158	62.7	168	59.4	163	149
Sm	20.1	8.1	23.8	3.2	10.10	8.10
Eu	4.91	1.90	5.12	0.53	1.33	1.15
Gd	12.4	4.8	14.8	0.8	3.0	2.8
Tb	1.4	0.7	1.6	0.1		
Dy	7.4	3.6	8.3	0.8	0.6	0.7
Ho	1.3	0.7	1.5	0.2		
Er	4.2	2.4	5.0	0.6	0.5	0.4
Tm	0.55	0.38	0.69	0.10		
Yb	3.5	2.5	4.5	0.9	0.4	0.3
Lu	0.50	0.36	0.64	0.15		

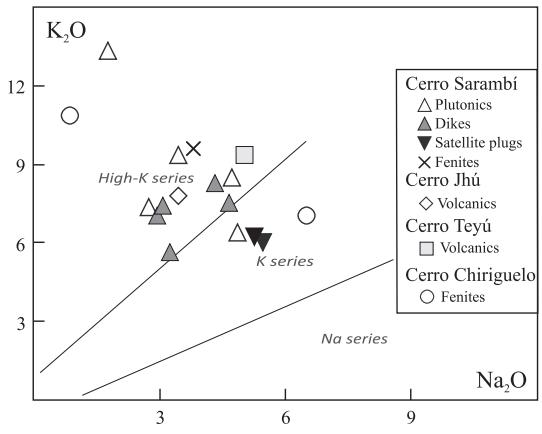

Fig. 6. K_2O vs. Na_2O diagram for the Amambay silicate rocks. Fields according to Middlemost (1975).

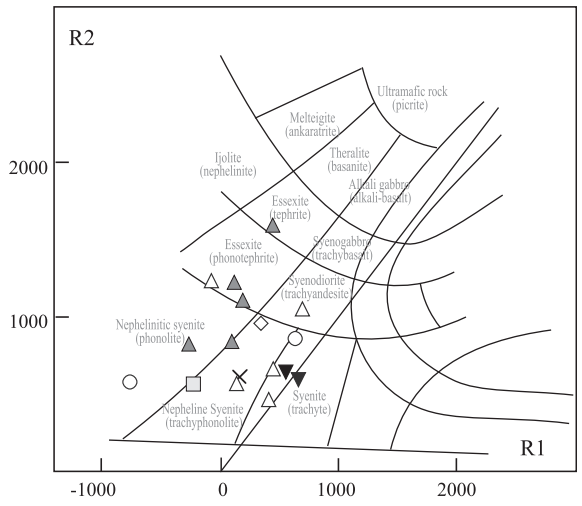

Fig. 7. Compositional variation diagrams for the Amambay silicate rocks in the De La Roche et al. (1980) diagram. Symbols as in Fig. 6.

shaped REE behavior, characteristic of some alkaline series, is thought to be related to the removal of titanite and apatite during crystallization (Gomes et al., 1987).

REE distribution for the Cerro Chiriguelo carbonatites shows steep LREE-enriched patterns with a decoupling of LREE from HREE and different slopes between Sm and Yb, and a strong Sm-Eu positive spike for the Cerro Sarambí carbonatites (Castorina et al., 1996).

8. Isotopic composition

8.1. Sr–Nd isotopes

The isotopic data for the silicate rocks from the Amambay area are reported in Table 8, with the initial ratios calculated assuming an Ar–Ar age of 138.9 Ma (Comin-Chiaramonti et al., 2007a).

The initial $^{87}Sr/^{86}Sr$ and $^{143}Nd/^{144}Nd$ ratios for the Cerro Sarambí potassic rocks (plutonics, volcanics, and plugs) vary from 0.70671 to 0.70792 and from 0.511574 to 0.511619, respectively. Castorina et al. (1996) reported values of $^{87}Sr/^{86}Sr$ and $^{143}Nd/^{144}Nd$ (0.70772 and 0.511699, respectively) within or close to the range shown by the silicate rocks from the complex for a carbonatite sample.

Initial $^{87}Sr/^{86}Sr$ and $^{143}Nd/^{144}Nd$ isotopic data for the other investigated potassic alkaline intrusions, Cerro Teyú (0.70744 and 0.511661, respectively) and Cerro Jhú (0.70746 and 0.511651, respectively), are in the same range of the Cerro Sarambí. The Cerro Chiriguelo carbonatites have similar ratios (0.70726–0.70732 and 0.511684–0.511688, respectively). Other $^{87}Sr/^{86}Sr$ and $^{143}Nd/^{144}Nd$ isotopic data (0.70722–0.70724 and 0.511739, respectively) listed by Castorina et al. (1996) for the Cerro Chiriguelo agree with the new values. Thus, the isotopic variations found for the Cerro Sarambí complex cover the entire range of values for the entire Amambay Province.

8.2. C–O and Pb isotopes

Data available in the literature for the Cerro Sarambí carbonatites and Cerro Chiriguelo silicate and carbonatitic rocks, including

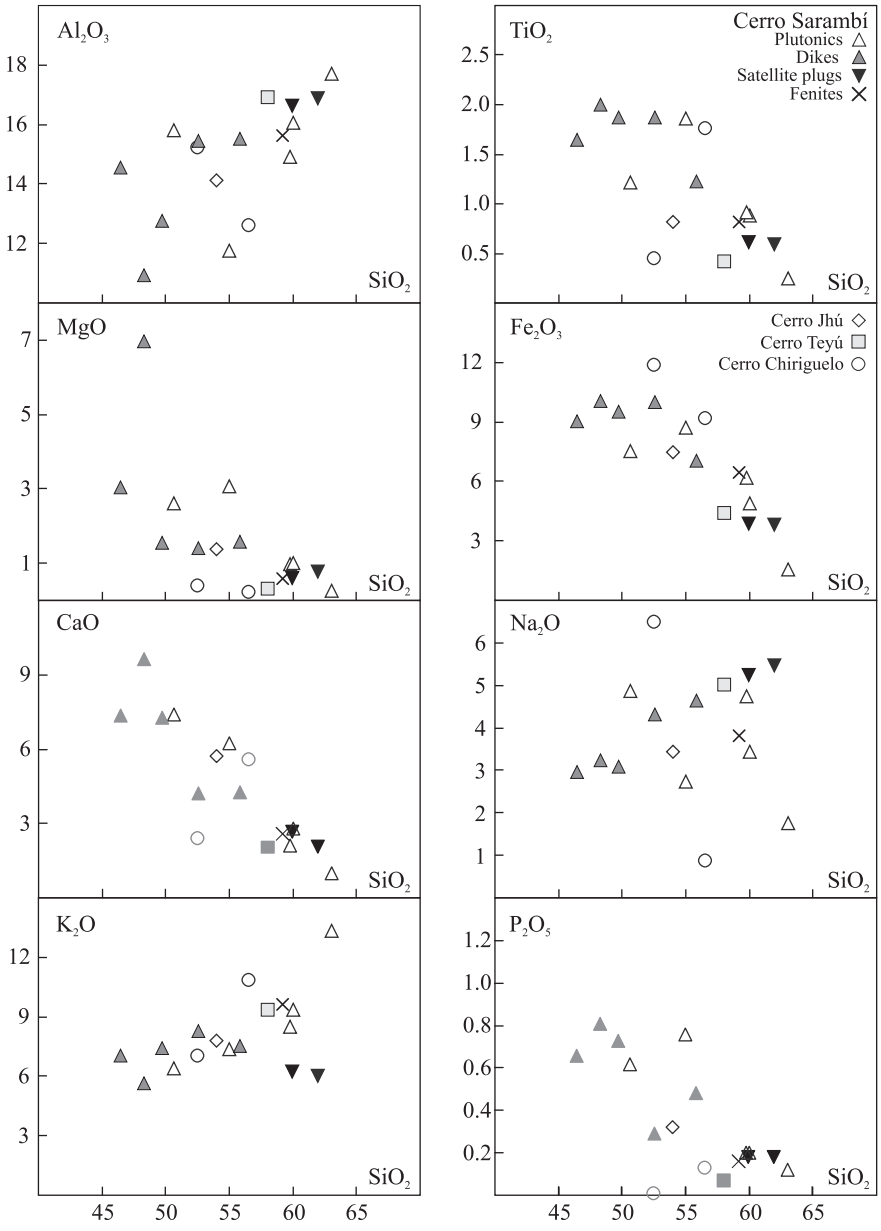

Fig. 8. Variation diagrams for the Amambay silicate rocks: major elements vs. SiO_2 concentration.

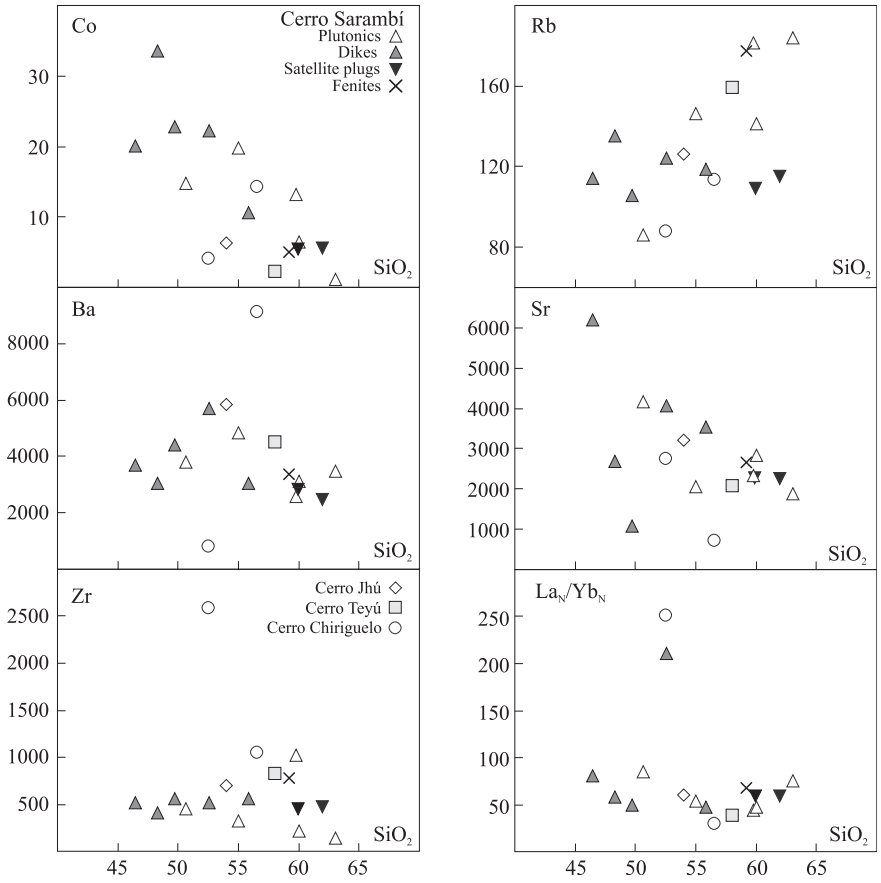

Fig. 9. Variation diagrams for Amambay silicate rocks: trace elements and La_N/Yb_N ratios vs. SiO_2 concentration.

surface and borehole samples, have been presented by Castorina et al. (1996, 1997) and Comin-Chiaramonti et al. (2005, 2007b). Data lie close to the primary carbonatite box, the trends, however, showing significant enrichment in heavy oxygen and carbon. These isotopic changes are interpreted as occurring in a hydrothermal environment at low temperatures, e.g., in the range 400–80 °C, and involving fluids with a CO_2/H_2O ratio ranging from 0.8 to 1.0.

The literature also includes the available Pb isotope data for the Amambay rocks, with Antonini et al. (2005) listing for the Cerro Chiriguelo carbonatites initial ratios of $^{206}Pb/^{204}Pb = 17.033$, $^{207}Pb/^{204}Pb = 15.506$, and $^{208}Pb/^{204}Pb = 37.465$, similar to those reported for the post-tholeiite potassic alkaline rocks from central-eastern Paraguay ($^{206}Pb/^{204}Pb = 16.888–17.702$, $^{207}Pb/^{204}Pb = 15.433–15.620$, and $^{208}Pb/^{204}Pb = 37.156–37.915$), and quite different in relation to a basanite occurring as dike near the city of Valle-mí in the Rio Apa Province ($^{206}Pb/^{204}Pb = 19.968$, $^{207}Pb/^{204}Pb = 15.641$, and $^{208}Pb/^{204}Pb = 38.589$). It should be also noted that the Early Cretaceous alkaline sodic rocks from the central and southern parts of the country have isotopic compositions ($^{206}Pb/^{204}Pb = 18.211$, $^{207}Pb/^{204}Pb = 15.682$, and $^{208}Pb/^{204}Pb = 37.963$) approaching those of the Cretaceous low-Ti of southern Paraná (Marques et al., 1999) but that are considerably different from their potassic analogs.

9. Magmatic evolution of the Cerro Sarambí complex

Geomorphologic and tectonic controls of the Amambay area indicate that the different rock types associated with the alkaline magmatism have crystallized in a very low lithosthatic pressure environment, i.e. near to the surface.

Petrographic features show that clinopyroxenes constitute an early crystallized phase in all the rock types. Temperature estimates of the clinopyroxene saturation in the melts (Putirka, 1999), based on whole rock composition similar to liquids and assuming an estimated pressure of 0.5 kbar were calculated for the rocks of Cerro Sarambí (Table 9). The results indicate a range of temperatures for the clinopyroxene-melt equilibria from 960 °C to 1060 °C for the plutonic suite, 1000 °C to 1130 °C for the dikes (the highest values associated with the mafic types), and 910 °C to 930 °C for the trachytic satellite plugs. Similar values were found for the Cerro Jhú and Cerro Teyú rocks. On the other extreme, the compositional variation of the nephelines indicates temperatures pointing to the final stages of crystallization close to 700 °C (cf. Hamilton, 1961), as shown in Fig. 5.

The most primitive rock from the Amambay area is evolved in respect to the primary compositions (mg# > 0.65 and Ni > 235 ppm) present in the Brazilian occurrences. It is represented by the Cerro Sarambí sample P37, a lamprophyric (minette) dike showing mg# = 0.58 and Ni = 30 ppm. Considering the range of temperatures associated with the different rock types, the possibility of deriving liquids similar to the Cerro Sarambí rock compositions starting from the lamprophyre has been tested. For this purpose, the Melts algorithm from Ghiorso and Sack (1995) was applied, using models based on thermodynamic calculations of equilibrium crystallization in isobaric conditions (0.5 kbar; Fig. 12). The models are assumed as reference lines of the progressive evolution of the liquid. The results allowed the possibility of reaching the evolved syenitic compositions from the lamprophyric liquid mainly as a consequence of the previous crystallization of great amounts of clinopyroxene and small amounts of olivine, spinel, and apatite (Table 10). The same models could be extended also to the volcanic types, which represent different levels of evolution from a similar starting composition.

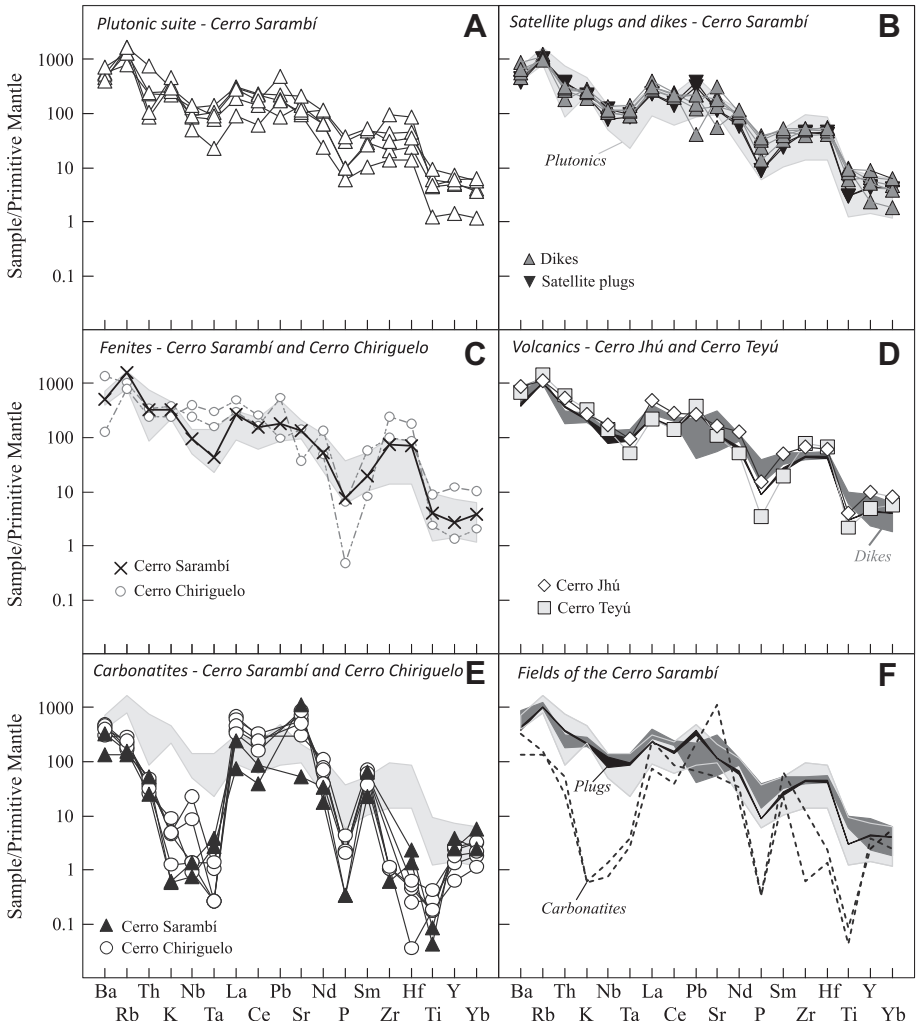

Fig. 10. Incompatible elements normalized to the primitive mantle (McDonough and Sun, 1995) for the Amambay rocks. In gray, the field for the Cerro Sarambí plutonics. Data source from this work and Castorina et al. (1996).

The clinopyroxene compositions also agree with these models. Considering a partition coefficient of iron and magnesium between clinopyroxene and melt ($Kd_{(Fe-Mg)} = 0.23$, Grove and Brian, 1983; $Kd = (Fe/Mg)_{cpx}/(Fe/Mg)_{liq}$), the calculated mg# values for the liquids seem to be in equilibrium with the composition of the clinopyroxene cores of the lamprophyric dike (Fig. 13). For the majority of the evolved samples, the mg# values of the liquids are lower than those of the most primitive clinopyroxene compositions. Thus, the early crystallized clinopyroxene cores of the plutonic suite and of other dikes and satellite plugs are believed to have grown up from less evolved magmas. This conclusion is consistent with the idea of having the lamprophyric dike as a parent melt and with the previous crystallization of great amounts of clinopyroxene before the liquid can reach the compositions of the evolved types. The occurrence of great amounts of clinopyroxenite in the complex, as postulated by Wiens (1991), seems to confirm this evolutionary model.

An origin for the complex from an ultrabasic peralkaline melt that, by a crystal fractionation process, led initially to the formation of cumulates (clinopyroxenites) and later evolved to a liquid of nepheline syenite composition was also suggested by Wiens (1991).

In Cerro Sarambí, non-primitive carbonatites and associated alkaline rocks are probably linked by liquid immiscibility and/or crystal fractionation processes. The carbonatites are interpreted as being derived by fractional crystallization from nepheline syenites, a process resulting in the production of a fluid-rich liquid that acted as the main fenitization agent, and that promoted the transformation of clinopyroxenites and the formation of other syenitic types. Trachytic dikes and plugs are related to subsequent phases of the magmatism. Wiens (1991) also stressed that clinopyroxenite xenoliths are commonly found in syenitic rocks.

In the $(SiO_2 + Al_2O_3) - (CaO + MgO + MnO + FeO^*) - (Na_2O + K_2O)$ system (Kjarsgaard and Hamilton, 1988), the rocks of the complex fall into the same compositional field of the Juquiá occurrence (Beccaluva et al., 1992), in agreement with experimental data resulting from the silicate edge of liquid immiscibility processes (Fig. 14). The observed tendency indicates an evolutionary trend with initial formation of lamprophyre, followed by that of syenitic and trachytic rocks and, after the immiscibility process, of calciocarbonatites.

For some Brazilian occurrences with similar rock associations to Cerro Sarambí, such as Jacupiranga and Juquiá (Melcher, 1966; Beccaluva et al., 1992; Ruberti et al., 2005), having ankaratritic and basanitic melts as parental magmas, respectively, and showing large amounts of cumulate intrusive rocks, the associated carbonatites are believed to have formed by the immiscibility of mixed silicate-carbonate liquids at the final stage of the magmatic evolution, after significant effects of crystal fractionation processes.

In a similar way, many Brazilian alkaline occurrences (Búzios Island, Alves, 1996; Juquiá, Beccaluva et al., 1992; Fortaleza, Macciotta

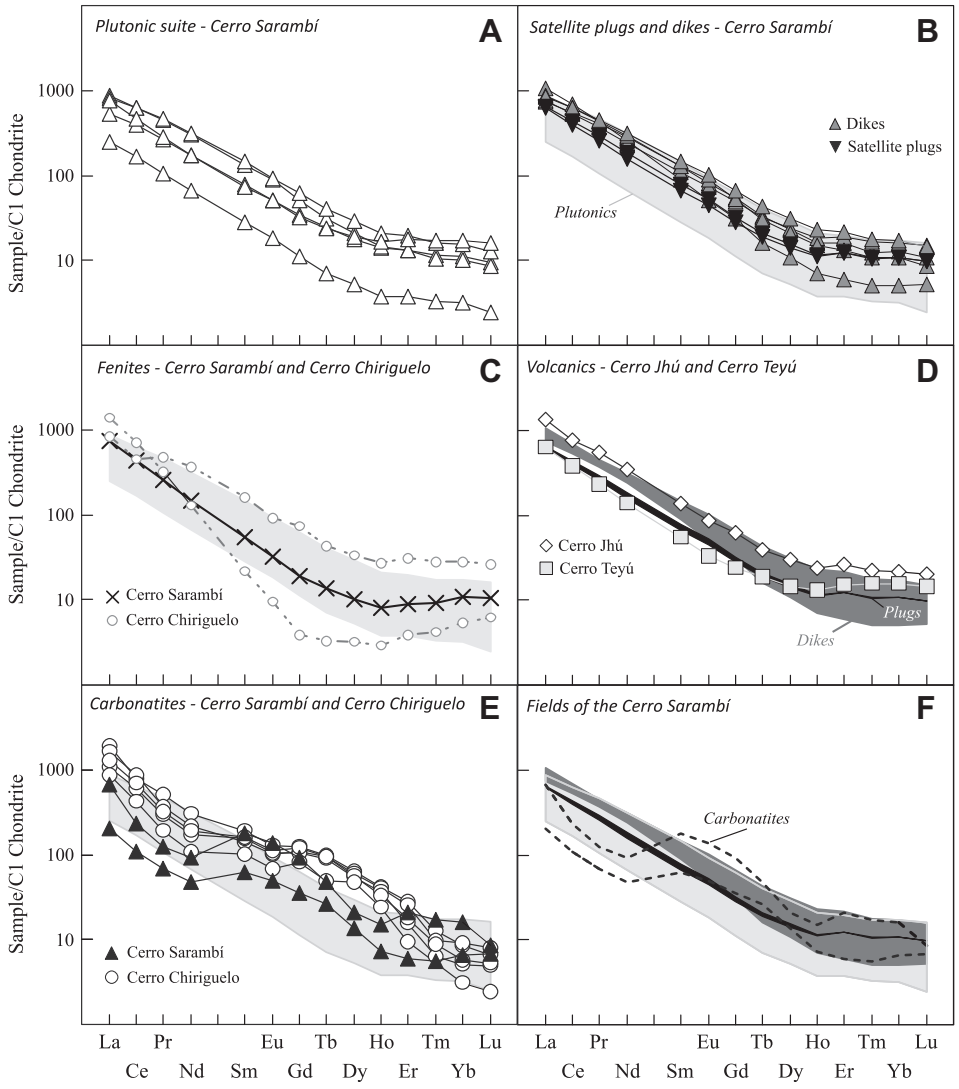

Fig. 11. REE normalized to chondrite (McDonough and Sun, 1995) patterns for the Amambay rocks. In gray, the field for the Cerro Sarambí plutonics. Data source from this work and Castorina et al. (1996).

Table 8
Sr and Nd isotope compositions, concentrations of trace elements (Rb, Sr, Sm and Nd) and model ages (T_{DM}) for the alkaline rocks from the Amambay area.

Locality	Rock type	Sample	Rb (ppm)	Sr (ppm)	Rb/Sr	$^{87}Sr/^{86}Sr$	Sri	Sm	Nd	Sm/Nd	$^{143}Nd/^{144}Nd$	Ndi	T_{DM} (Ma)
Cerro Sarambí	mnsy	P41	86.04	3690.86	0.0650	0.70684	0.70671	18.08	142.70	0.0766	0.511671	0.511601	1525
	sd	P49	146.36	2257.83	0.1876	0.70831	0.70794	20.62	153.75	0.0811	0.511676	0.511602	1571
	sy	P46	188.02	1979.16	0.2750	0.70785	0.70731	4.16	33.29	0.0756	0.511643	0.511574	1545
	sy	P39	140.41	2531.93	0.1605	0.70811	0.70779	11.22	85.74	0.0792	0.511655	0.511583	1572
	nsy	P68	199.02	2359.16	0.2442	0.70807	0.70759	10.15	81.60	0.0752	0.511654	0.511586	1529
	fen	Pa43	169.78	2666.43	0.1843	0.70792	0.70756	7.40	69.02	0.0648	0.511657	0.511598	1419
	min	P37	136.64	2886.91	0.1370	0.70743	0.70716	17.99	134.25	0.081	0.511693	0.511619	1550
	trph	P52	103.17	3725.36	0.0801	0.70796	0.70780	16.13	120.94	0.0807	0.511671	0.511598	1571
	pht	P56	91.27	6248.97	0.0423	0.70721	0.70713	18.25	144.65	0.0763	0.511653	0.511584	1542
	pht	P61	81.62	1035.77	0.2281	0.70837	0.70792	20.89	151.96	0.0831	0.511653	0.511577	1622
	ph	P45	128.28	4245.43	0.0874	0.70757	0.70740	13.02	123.03	0.064	0.511653	0.511595	1415
	tr	P34	109.66	2082.22	0.1524	0.70770	0.70740	10.84	88.33	0.0742	0.511659	0.511592	1512
	tr	P04	119.07	2273.77	0.1516	0.70782	0.70752	9.62	78.12	0.0745	0.511701	0.511633	1469
Cerro Jhú	trph	P11	130.4	3302.42	0.1143	0.70767	0.70744	18.97	165.97	0.0691	0.511724	0.511661	1391
Cerro Teyú	trph	P17	165.13	2113.3	0.2262	0.70791	0.70746	7.83	67.93	0.0697	0.511714	0.511651	1407
Cerro Chiriguelo	fen	P28	117.18	724.77	0.4680	0.70954	0.70862	21.95	171.36	0.0775	0.511749	0.511679	1447
	fen	P30	88.88	3062.86	0.0840	0.70824	0.70807	3.08	63.34	0.0294	0.511693	0.511666	1119
	cc	P26	55.31	37277.46	0.0043	0.70727	0.70726	7.77	154.29	0.0304	0.511712	0.511684	1110
	cc	P24	6.3	3867.12	0.0047	0.70733	0.70732	9.23	164.73	0.0339	0.511719	0.511688	1125

Table 9
Calculated temperatures of clinopyroxene-melt equilibria based on whole rock chemical compositions (cf. Table 6) following Putirka (1999). Also shown is the range of mg# values for the equilibrium liquids calculated of clinopyroxene analyses from Cerro Sarambí. mg# of whole rock analyses is included for comparison.

	Cerro Sarambí										Cerro Jhú	Cerro Teyú
	Plutonic rocks				Dikes			Satellite plugs				
Sample	P41	P49	P39	P68	P37	P52	P56	P45	P34	P4	P11	P17
Rock type	mnsy	sd	sy	nsy	min	trph	pht	ph	tr	tr	trph	trph
T_{sat} px (°C)	1040	1063	959	973	1133	1006	1076	1019	910	930	993	873
P (kbar)	0.5	0.5	0.5	0.5	0.5	0.5	0.5	0.5	0.5	0.5	0.5	0.5
mg#(liq)$_{calc.}$	47.7–25.5	40.6–25.9	14.0–12.3	31.6–23.9	63.0–25.5	42.5–40.2	46.8–33.5	14.1–12.3	36.9–32.9	35.7–30.5	18.7–13.7	19.3–16.2
mg# (wr)	40.7	41.0	29.3	24.0	57.9	30.8	39.9	21.7	24.0	28.5	26.7	12.2

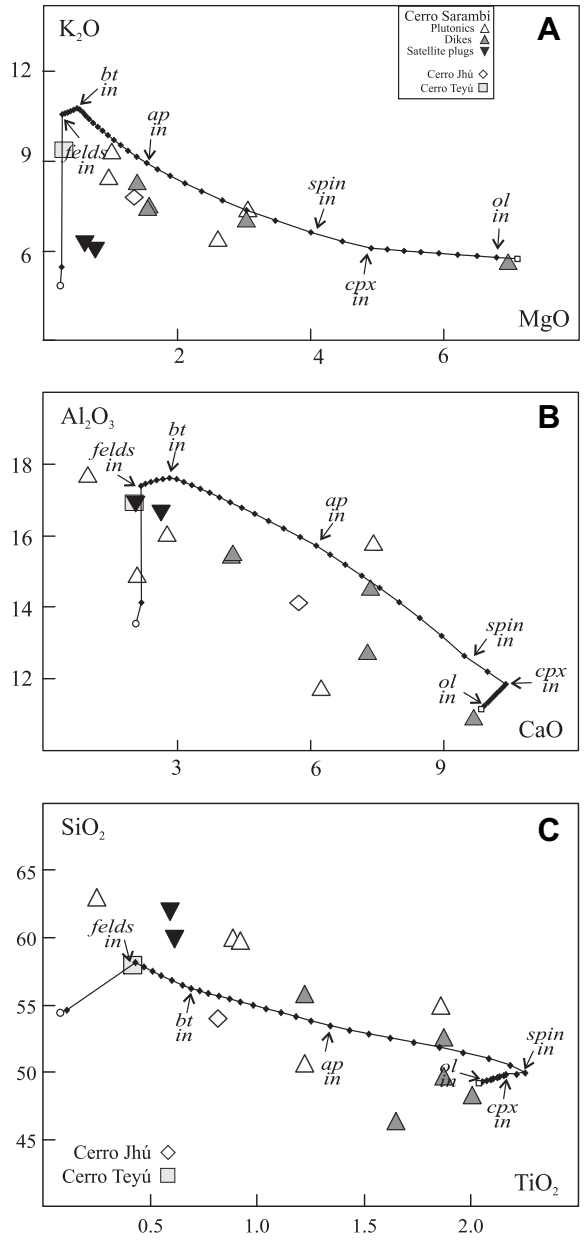

Fig. 12. Variation diagrams of major elements of whole rock compositions from the Cerro Sarambí complex compared to thermodynamical models of equilibrium crystallization from a lamprophyric liquid obtained from Melts algorithm (Ghiorso and Sack, 1995): A) K_2O vs. MgO, B) Al_2O_3 vs. CaO and C) SiO_2 vs. TiO_2. In these models, small blank squares and circles represent the starting (1235 °C) and ending (855 °C) modeled temperatures, respectively. The starting composition is taken from the calculated liquid nearest to the lamprophyric dike (P37) in isobaric conditions (0.5 kbar). Steps of the model (small black diamonds) represent the composition of the liquid lowering T in 10 °C in the crystallization system. The steps of the first appearance of the main minerals in the system (mineral in) are also indicated. Abbreviations: ap, apatite; bt, biotite; cpx, clinopyroxene; felds, feldspar; ol, olivine; spin, spinel.

et al., 1990; Lages, Traversa et al., 1996; Monte de Trigo Island, Enrich, 2005; Morro Redondo, Brotzu et al., 1989; Passa Quatro, Brotzu et al., 1992, Piratini, Barbieri et al., 1987; Ponte Nova, Azzone, 2008; São Sebastião Island, Bellieni et al., 1990) are believed to have been generated from a parental magma with the same characteristics. In Juquiá, mass-balance calculations performed by Beccaluva et al. (1992) allowed the formation of different rock types by successive fractionation stages starting from lamprophyric basanites that occur as small dikes in some localities inside and outside the complex.

Table 10
Representative steps of the thermodynamic model of equilibrium crystallization calculated by the Melts algorithm (Ghiorso and Sack, 1995) from a lamprophyric liquid similar to sample P37. The starting composition is found in isobaric conditions (0.5 kbar) and assumes initial fO_2 conditions equal to the QFM buffer.

T (°C)	1235	1225	1155	1145	1135	1105	1045	975	925	875	865
fO_2 (ΔQFM)	0	0.05	0.14	0.11	−0.01	−1.35	−2.9	−3.73	−4.03	−4.59	−3.55
SiO_2	49.21	49.29	49.82	49.83	49.94	51.44	53.44	55.45	56.47	58.16	54.61
TiO_2	2.04	2.05	2.16	2.21	2.25	1.96	1.34	0.87	0.65	0.43	0.11
Al_2O_3	11.14	11.23	11.83	12.18	12.62	14.12	15.94	17.18	17.59	17.37	14.11
Fe_2O_3	1.98	1.99	2.1	2.07	1.97	0.98	0.37	0.17	0.12	0.08	0.44
FeO	7.43	7.37	6.85	6.84	6.79	5.77	3.96	2.47	1.75	1.47	4.19
MnO	0.15	0.15	0.14	0.14	0.14	0.15	0.15	0.13	0.11	0.13	0.28
MgO	7.09	6.78	4.91	4.48	4.01	2.69	1.41	0.76	0.52	0.3	0.29
CaO	9.82	9.89	10.37	9.96	9.44	7.98	5.76	3.73	2.83	2.19	2.2
Na_2O	3.31	3.34	3.51	3.64	3.81	4.4	5.18	5.74	6	6.49	13.62
K_2O	5.74	5.78	6.09	6.32	6.62	7.69	9.15	10.28	10.77	10.57	5.46
P_2O_5	0.83	0.83	0.88	0.91	0.95	1.11	1.26	0.96	0.85	0.76	0.53
H_2O	1.27	1.28	1.35	1.4	1.47	1.71	2.03	2.26	2.34	2.06	4.16
Proportion of phases in the system											
Liquid	100	99.2	94.2	90.8	86.7	74.6	62.7	55.7	52.6	47.5	19.3
Olivine		0.8	5.8	6.1	6.3	6.7	6.8	7.2	7.3	4.3	3.1
Clinopyroxene				3.1	6.9	16.5	26.5	31.9	34.1	36.2	36.7
Spinel					0.1	2.2	3.9	4.5	4.5	4.5	3.8
Apatite							0.1	0.7	0.9	1.1	1.7
Biotite									0.6	6.4	10.3
Feldspar											25.1

10. Insights to the mantle source of the Amambay area

The potassic alkaline and carbonatitic magmatism of the Cerro Sarambí complex and the entire Amambay region indicates an enriched mantle source. Typically, the SiO_2-undersaturated alkaline primitive magmas have their genesis attributed to the influence of CO_2 on a peridotitic source (Eggler, 1978; Wyllie, 1995; Dasgupta et al., 2007). Moreover, the potassium enrichment in these melts suggests the presence of phlogopite-rich metasomatic veins in a lithosphere mantle source (Foley, 1992; Comin-Chiaramonti et al., 1997; Grégoire et al., 2002).

The Amambay silicate and carbonatitic rocks have high Sr_i and low-Nd_i ratios and fall into the enriched quadrant of the $^{87}Sr/^{86}Sr$ vs. $^{143}Nd/^{144}Nd$ diagram (Fig. 15). On the whole, the data follow a trend similar to that of the low-Nd array of Hart and Zindler (1989), also referred to as the "Paraguay array" by Comin-Chiaramonti et al. (1995), which involves depleted and enriched mantle components and is a characteristic feature of the sodic and potassic alkaline rock associations from Eastern Paraguay. The Amambay carbonatites also lie in the Early Cretaceous pre-tholeiitic potassic alkaline rocks field. Based on their Sr and Nd contents, Comin-Chiaramonti et al. (1997) consider the Eastern Paraguay alkaline rocks crustally uncontaminated and, as a result, representative of the isotopic composition of the mantle source.

Nd-depleted mantle values (T_{DM}, cf. DePaolo, 1988) provide a broad indication of the age of the main enrichment processes affecting the mantle source(s) of Paraguayan magmas. In general, the Amambay potassic magmas have ages comparable to those of the Paraná-Angola-Etendeka tholeiites and higher than those of sodic magmas (Comin-Chiaramonti et al., 2007a). Model ages for the alkaline rocks and carbonatites from the Amambay area (i.e. Amambay Province), ranging from 1.6 to 1.1 Ga, are listed in Table 8,

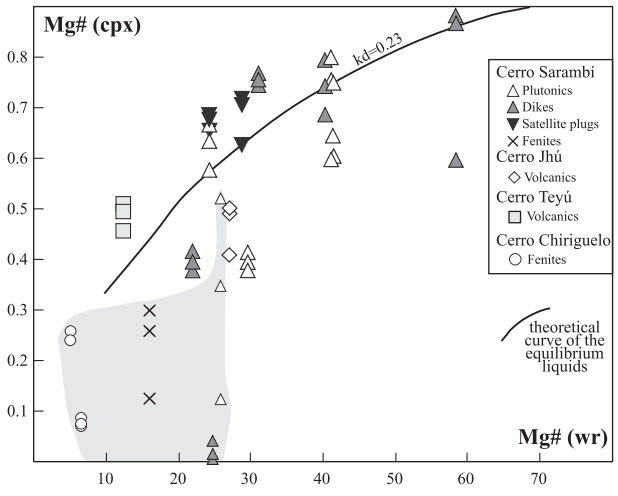

Fig. 13. mg# of whole rock compositions vs. coexisting clinopyroxenes {$mg\#_{wr} = MgO/(MgO + FeO_T)$ and $mg\#_{cpx} = Mg/(Mg + Fe_T)$, in molecular proportions}. Gray field represents samples influenced by metassomatic processes.

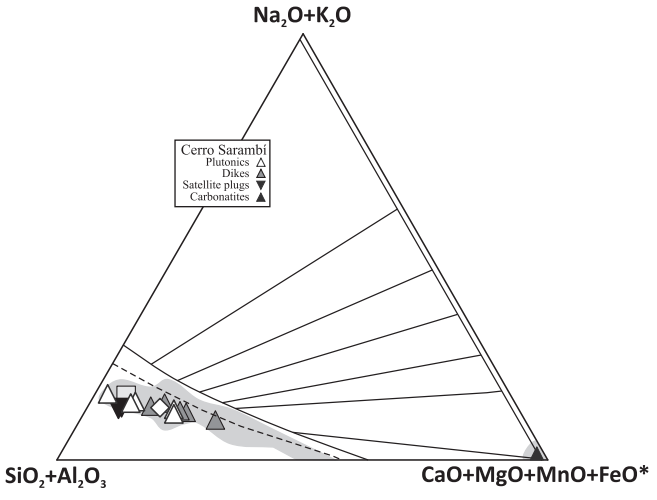

Fig. 14. $(SiO_2 + Al_2O_3) - (Na_2O + K_2O) - (CaO + MgO + FeO^* + MnO)$ experimental system (Kjarsgaard and Hamilton, 1988) showing the carbonate-silicate liquid immiscibility. The silicate edge of immiscibility at 0.5 GPa (bold continuous line) and 0.8 GPa (dashed line) and the experimentally determined tie-lines to different carbonatite compositions are indicated. FeO*, all iron expressed as oxide. Compositions of the Cerro Sarambí carbonatites are from Castorina et al. (1996). For comparison, gray fields indicate silicate and carbonatitic rocks from the Brazilian Juquiá complex (Beccaluva et al., 1992).

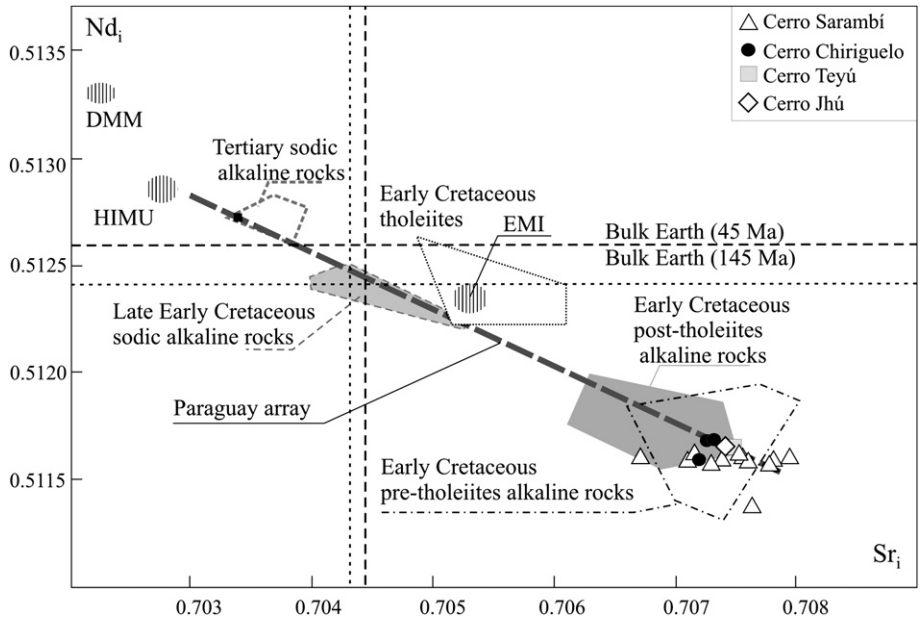

Fig. 15. Sr and Nd isotope data of Amambay rocks plotted into the initial $^{87}Sr/^{86}Sr$ (Sr_i) vs. $^{143}Nd/^{144}Nd$ (Nd_i) diagram for Early Cretaceous to Tertiary magmatic rocks of Eastern Paraguay (after Antonini et al., 2005). DMM, HIMU and EMI fields after Hart and Zindler (1989). Paraguay array: $Nd_i = -0.23255Sr_i + 0.6763$; $r = -0.84$ (Comin-Chiaramonti et al., 1995).

with the values for the Cerro Sarambí samples lying mostly in the 1.6–1.4 Ga interval. According to these authors, the pre-tholeiitic potassic alkaline rocks (Amambay and Rio Apa Provinces at northeastern and northern Paraguay, respectively) show two peaks of model ages at 1.4 and 1.1 Ga, for $f \approx -0.5$ to -0.7, respectively. A similar value to that of the Amambay silicate rocks is suggested for their associated carbonatites. The post-tholeiitic potassic alkaline complexes and dikes (Central Province at central-eastern Paraguay) yielded a mean T_{DM} value of 1.7 Ga, for $f \approx -0.4$ to -0.5, suggesting an increase in age from pre-tholeiitic to post-tholeiitic rocks, i.e. from north to south of Eastern Paraguay. The Paraná low-Ti tholeiites have a major variation in Nd model ages, 2.8–0.7 Ga, for $f \approx -0.5$, whereas the interval for the high-Ti tholeiites is narrower, 1.4–0.9 Ga, for $f \approx -0.5$, with values increasing from north to south and from west to east. The youngest data in Eastern Paraguay is related to the sodic alkaline magmatism that occurs in three areas of the country (northern, central, and southern, corresponding to the Alto Paraguay, Asunción, and Misiones Provinces, respectively) and give ages varying from 1.0 to 0.6 Ga (0.9, 0.6 and 1.0 Ga, for $f \approx -0.4$ to -0.5, respectively). Such large differences in ages shown by the Paraguayan rocks have been interpreted by the previous authors as indicating that isotopically distinct magmas were generated following two enrichment events of the subcontinental upper mantle estimated at 2.0–1.4 Ga (Paleo-Mesoproterozoic) and 1.0–0.5 Ga (Neoproterozoic). These metasomatic events, chemically distinct as suggested by strong differences in Ti, LILE, and HFSE concentrations, may have occurred as a precursor to the genesis of tholeiitic and alkaline magmatism in the Paraná basin.

Based on Sr–Nd–Pb isotopic data, Antonini et al. (2005) concluded that two mantle components could have been involved in the genesis of the Cretaceous (potassic alkaline pre- and post-tholeiites and Serra Geral Formation tholeiites) and late Early Cretaceous to Tertiary (sodic alkaline) magmatism of Eastern Paraguay. An extreme and heterogeneous EMI component appears to be prevalent in the potassic alkaline magmatism, while an HIMU component seems to have been more important in the sodic magmatism.

11. Concluding remarks

The Early Cretaceous alkaline magmatism of the Amambay Province comprises intrusive to extrusive rocks of variable composition.

- This magmatism, intruding into the Precambrian basement and doming the overlying Paleozoic and Mesozoic sedimentary strata, precedes the tholeiitic basalts of the Serra Geral Formation, as indicated by field evidence and confirmed by radiometric data.
- The magmatism is structurally controlled by the NE-trending Ponta Porã Arch and placed between the NW-trending Bella Vista and Mbaracayú tectonic depressions, as shown on the Bouguer gravimetric map.
- The ring-like carbonatite complexes of Cerro Sarambí and Cerro Chiriguelo are the most outstanding representatives of this magmatic activity.
- Ultramafic-mafic, syenitic, and carbonatitic rock associations are prevalent, but fenites are also found in association with the carbonatites. Alkali feldspars and clinopyroxenes of variable composition are the most abundant minerals; other phases are feldspathoids, micas (biotite), and melanite in addition to Fe–Ti oxides as more common accessories.
- Chemically, the non-cumulate intrusive silicate rocks are potassic to highly potassic and mainly of syenitic composition; the cumulates are represented mostly by clinopyroxenites and shonkinites. Fine-grained rocks are of syenitic or a more basic composition, while the carbonatites are dominantly calciocarbonatites.
- Multielemental diagrams, normalized to a primitive mantle composition, display positive anomalies for Rb, La, Pb, Sr, and Sm, and negative ones for Nb–Ta, P, and Ti, the latter more accentuated in the carbonatites. However, the diagrams for the rare earth elements normalized to chondrite indicate high concentration levels of REE and strong LREE/HREE fractionation. In general, the patterns for both series of elements

exhibit great affinities with those of the Early Cretaceous (post-tholeiites) alkaline potassic rocks from the central-eastern region of Paraguay (Central Province, Asunción-Sapucai rift, ASU), as shown in Comin-Chiaramonti et al. (1997).

- The Amambay silicate rocks, excluding the Cerro Chiriguelo fenites, yielded initial (138.9 Ma) $^{87}Sr/^{86}Sr$ and $^{143}Nd/^{144}Nd$ isotopic ratios within the ranges 0.70671–0.70792 and 0.511574–0.511661, respectively. The Cerro Chiriguelo carbonatites showed almost identical values, 0.70726–0.70732 and 0.51684–0.51688, respectively, compared to those of the associated silicate rocks. This similarity is also present in other carbonatitic occurrences from the Paraná-Angola-Namibia system (Comin-Chiaramonti et al., 2007b). In the conventional Sr and Nd initial ratios diagram, both rock types having high-Sr_i and low-Nd_i values fall into the enriched quadrant and on the same general line of the alkaline potassic rocks from the ASU, but trend to a more radiogenic area. This line is a continuation of the low-Nd array of Hart and Zindler (1989) that links depleted and enriched mantle components.
- T_{DM} model ages for the Amambay silicate and carbonatitic rocks, potassic alkaline rocks from the central-eastern areas, as well as H- and L-Ti tholeiites from the Paraná basin range from 1.6 to 1.1 Ga and seem to be associated with the Paleo-Mesoproterozoic event of metasomatic enrichment of the mantle, estimated at 2.0–1.4 Ga by Comin-Chiaramonti et al. (1997). However, the ages are higher than those given by the Paraguayan late Early Cretaceous and Tertiary sodic rocks, which are believed to be associated with the Neoproterozoic mantle enrichment event of these authors.
- Petrographical and chemical data for rocks and minerals indicate that fractional crystallization and accumulation of mafic phases, possibly combined with liquid immiscibility processes, have played an important role in the origin and evolution of the Cerro Sarambí complex. Calculations agree with the derivation of these rocks from a parental magma of lamprophyric (minette) composition.

Acknowledgments

Most of the analytical data included in this paper are taken from the monograph presented by G.S. Paula for the graduation degree in Geology at the Institute of Geosciences. The authors thank Prof. Horstpeter Ulbrich for reviewing the paper and Fapesp (Procs. 07/57461-9 and 10/50887-3, CBG; 2008/03807-4, RGA) for financial support. We also thank the anonymous reviewers for their critical and helpful suggestions to improve the manuscript.

References

Alves, F.R., 1996. Contribuição ao conhecimento geológico e petrológico da Ilha de Búzios, SP. Ph.D. Thesis, Institute of Geosciences, University of São Paulo, 274 p. (unpublished).

Antonini, P., Gasparon, G., Comin-Chiaramonti, P., Gomes, C.B., 2005. Post-paleozoic magmatism in eastern Paraguay: Sr–Nd–Pb isotope compositions. In: Comin-Chiaramonti, P., Gomes, C.B. (Eds.), Mesozoic to Cenozoic Alkaline Magmatism in the Brazilian Platform. Edusp/Fapesp, São Paulo, pp. 57–69.

Azzone, R.G., 2008. Petrogênese do maciço alcalino máfico-ultramáfico Ponte Nova (MG-SP). Ph.D. Thesis, Institute of Geosciences, University of São Paulo, 372 p. (unpublished).

Azzone, R.G., Ruberti, E., Enrich, G.E.R., Gomes, C.B., 2009. Zr- and Ba-rich minerals from the Ponte Nova alkaline mafic-ultramafic massif, southeastern Brazil: indication of an enriched mantle source. Canadian Mineralogist 47, 1087–1103.

Barbieri, M., Beccaluva, L., Brotzu, P., Conte, A., Garbarino, C., Gomes, C.B., Loss, E.I., Macciotta, G., Morbidelli, L., Scheibe, L.F., Tamura, R.M., Traversa, G., 1987. Petrological and geochemical studies of alkaline rocks from continental Brazil; 1, The phonolite suite from Piratini, RS. Geochimica Brasiliensis 1, 109–138.

Bastin, G.F., Heiligers, H.J.M., 1990. Progress in microprobe analysis. Materialwissenschaft und Werkstofftechnik 21, 90–92.

Beccaluva, L., Barbieri, M., Born, H., Brotzu, P., Coltorti, M., Conte, A.M., Garbarino, C., Gomes, C.B., Macciotta, G., Morbidelli, L., Ruberti, E., Siena, F., Traversa, G., 1992. Fractional crystallization and liquid immiscibility processes in the alkaline-carbonatite complex of Juquiá (São Paulo, Brazil). Journal of Petrology 33, 1371–1404.

Bellieni, G., Montes-Lauar, C.B., De Min, A., Piccirillo, E.M., Cavazzini, G., Melfi, A.J., Pacca, I.G., 1990. Early and Late Cretaceous magmatism from São Sebastião Island (SE-Brazil): geochemistry and petrology. Geochimica Brasiliensis 4, 59–83.

Brigatti, M.F., Guggenheim, S., 2002. Mica crystal chemistry and the influence of pressure, temperature, and solid solution on atomistic models. Reviews in Mineralogy and Geochemistry 46, 1–97.

Brod, J.A., Gaspar, J.C., Araújo, D.P., Gibson, S.A., Thompson, R.N., Junqueira-Brod, T., 2001. Phlogopite and tetra-ferriphlogopite from Brazilian carbonatite complexes: petrogenetic constraints and implication for mineral-chemistry systematics. Journal of Asian Earth Sciences 19, 265–296.

Brotzu, P., Barbieri, M., Beccaluva, L., Garbarino, C., Gomes, C.B., Macciotta, G., Melluso, L., Morbidelli, L., Ruberti, E., Sígolo, J.B., 1992. Petrology and geochemistry of the Passa Quatro alkaline complex, MG-RJ-SP, Brazil. Journal of South American Earth Sciences 6, 237–252.

Brotzu, P., Beccaluva, L., Conte, A.M., Fonseca, M., Garbarino, C., Gomes, C.B., Leong, R., Macciotta, G., Mansur, R.L., Melluso, L., Morbidelli, L., Ruberti, E., Sígolo, J.B., Traversa, G., Valença, J.G., 1989. Petrological and geochemical studies of alkaline rocks from continental Brazil. 8. The syenitic intrusion of Morro Redondo, RJ. Geochimica Brasiliensis 3, 63–80.

Brotzu, P., Gomes, C.B., Melluso, L., Morbidelli, L., Morra, V., Ruberti, E., 1997. Petrogenesis of coexisting SiO_2-undersaturated to SiO_2-oversaturated felsic igneous rocks: the alkaline complex of Itatiaia, southeastern Brazil. Lithos 40, 133–156.

Brotzu, P., Melluso, L., Bennio, L., Gomes, C.B., Lustrino, M., Morbidelli, L., Morra, V., Ruberti, E., Tassinari, C.C.G., D'Antonio, M., 2007. Petrogenesis of the Early Cenozoic potassic alkaline complex of Morro de São João, southeastern Brazil. Journal of South American Earth Sciences 24, 93–115.

Castorina, F., Censi, P., Barbieri, M., Comin-Chiaramonti, P., Cundari, A., Gomes, C.B., Pardini, G., 1996. Carbonatites from Eastern Paraguay: a comparison with coeval carbonatites from Brazil and Angola. In: Comin-Chiaramonti, P., Gomes, C.B. (Eds.), Alkaline Magmatism in Central-Eastern Paraguay. Relationships with Coeval Magmatism in Brazil. Edusp/Fapesp, São Paulo, pp. 231–248.

Castorina, F., Censi, P., Comin-Chiaramonti, P., Gomes, C.B., Piccirillo, E.M., Alcover Neto, A., Almeida, R.T., Speziale, S., Toledo, M.C., 1997. Geochemistry of carbonatites from Eastern Paraguay and genetic relationships with potassic magmatism: C, O, Sr and Nd isotopes. Mineralogy and Petrology 61, 237–260.

Censi, P., Comin-Chiaramonti, P., Demarchi, G., Longinelli, A., Orué, D., 1989. Geochemistry and C–O isotopes of the Chiriguelo carbonatite, northeastern Paraguay. Journal of South American Earth Sciences 3, 295–303.

Comin-Chiaramonti, P., Castorina, F., Cundari, A., Petrini, R., Gomes, C.B., 1995. Dykes and sills from Eastern Paraguay: Sr and Nd isotope systematics. In: Baer, G., Heimann, A. (Eds.), Physics and Chemistry of Dykes. Bakelma, Rotterdam, pp. 267–278.

Comin-Chiaramonti, P., Cundari, A., DeGraff, J.M., Gomes, C.B., Piccirillo, E.M., 1999. Early Cretaceous-tertiary magmatism in Eastern Paraguay (western Paraná basin): geological, geophysical and geochemical relationships. Journal of Geodynamics 28, 375–391.

Comin-Chiaramonti, P., Cundari, A., Piccirillo, E.M., Gomes, C.B., Castorina, F., Cens, P., De Min, A., Marzol, A., Speziale, S., Velázquez, V.F., 1997. Potassic and sodic igneous rocks from Eastern Paraguay: their origin from the lithospheric mantle and genetic relationships with the associated Paraná tholeiites. Journal of Petrology 38, 495–528.

Comin-Chiaramonti, P., Gomes, C.B., Cundari, A., Castorina, F., Censi, P., 2007b. A review of carbonatitic magmatism in the Paraná-Angola-Etendeka (PAN) system. In: Castelli, D., Compagnoni, R. (Eds.), Special Issue in Honour of Ezio Callegari. Periodico di Mineralogia, vol. 76, pp. 25–78.

Comin-Chiaramonti, P., Gomes, C.B., Marques, L.S., Censi, P., Ruberti, E., Antonini, P., 2005. Carbonatites from Southeastern Brazil: geochemistry, O–C, Sr–Nd–Pb isotopes and relationships with the magmatism from the Paraná-Angola-Namibia Province. In: Comin-Chiaramonti, P., Gomes, C.B. (Eds.), Mesozoic to Cenozoic Alkaline Magmatism in the Brazilian Platform. Edusp/Fapesp, São Paulo, pp. 657–688.

Comin-Chiaramonti, P., Marzoli, A., Gomes, C.B., Milan, A., Riccomini, C., Velázquez, V.F., Mantovani, M.M.S., Renne, P., Tassinari, C.C.G., Vasconcelos, P.M., 2007a. The origin of post-Paleozoic magmatism in eastern Paraguay. In: Foulger, G.R., Jurdy, D.M. (Eds.), Plates, Plumes, and Planetary Processes. Geological Society of America, Special Paper, 430, pp. 603–633.

Comte, D., Hasui, Y., 1971. Geochronology of Eastern Paraguay by the potassium-argon method. Revista Brasileira de Geociências 1, 33–43.

Dasgupta, R., Hirschmann, M.M., Smith, N.D., 2007. Partial melting experiments of peridotite + CO_2 at 3 GPa and genesis of alkalic ocean islands basalts. Journal of Petrology 48, 2093–2124.

De La Roche, H., Leterrier, J., Grandclaude, P., Marchal, M., 1980. A classification of volcanic and plutonic rocks using R1–R2 diagrams and major element analyses – its relationships and current nomenclature. Chemical Geology 29, 183–210.

DePaolo, D.J., 1988. Neodymium isotope geochemistry. An introduction. Minerals and Rocks 20, 1–87.

Dollase, W.A., Thomas, W.M., 1978. The crystal chemistry of silica-rich, alkali-deficient nepheline. Contributions to Mineralogy and Petrology 66, 311–318.

Droop, G.T.R., 1987. A general equation for estimating Fe^{3+} concentrations in ferromagnesian silicates and oxides from microprobe analyses, using stoichiometric criteria. Mineralogical Magazine 51, 431–435.

Eby, G.N., Mariano, A.N., 1986. Geology and geochronology of carbonatites peripheral to the Paraná Basin. In: Carbonatites Symposium, Ottawa, pp. 1–13.
Eby, G.N., Mariano, A.N., 1992. Geology and geochronology of carbonatites and associated alkaline rocks peripheral to the Paraná Basin, Brazil-Paraguay. Journal of South American Earth Sciences 6, 207–216.
Eggler, D.H., 1978. The effect of CO_2 upon partial melting of peridotite in the system Na_2O–CaO–Al_2O_3–MgO–SiO_2–CO_2 to 35 Kb, with an analysis of melting in a peridotite–H_2O–CO_2 system. American Journal of Sciences 278, 305–343.
Enrich, G.E.R., 2005. Petrogênese da suite alcalina da Ilha de Monte de Trigo, SP. Ph.D. Thesis, Institute of Geosciences, University of São Paulo, 229 p. (unpublished).
Foley, S.F., 1992. Vein-plus-wall-rock melting mechanisms in the lithosphere and the origin of potassic alkaline magmas. Lithos 28, 435–453.
Furtado, S.M., Gomes, C.B., 1994. Caracterização química dos clinopiroxênios do maciço alcalino de Anitápolis, SC. Geochimica Brasiliensis 8, 65–78.
Ghiorso, M.S., Sack, R.O., 1995. Chemical mass transfer in magmatic processes. IV. A revised and internally consistent thermodynamic model for the interpolation and extrapolation of liquid-solid equilibria in magmatic systems at elevated temperatures and pressures. Contributions to Mineralogy and Petrology 119, 197–212.
Gibson, S.A., Thompson, R.N., Day, J.A., 2006. Timescales and mechanisms of plume-lithosphere interactions: $^{40}Ar/^{39}Ar$ geochronology and geochemistry of alkaline igneous rocks from the Paraná–Etendeka large igneous province. Earth and Planetary Science Letters 251, 1–17.
Gibson, S.A., Thompson, R.N., Leonardos, O.H., Dickin, A.P., Mitchell, J.G., 1995. The Late Cretaceous impact of the Trindade mantle plume: evidence from large-volume, mafic, potassic magmatism in SE Brazil. Journal of Petrology 36, 189–229.
Gomes, C.B., Barbieri, M., Beccaluva, L., Brotzu, P., Conte, A., Garbarino, C., Macciotta, G., Melluso, L., Morbidelli, L., Ruberti, E., Scheibe, L.F., Tamura, R.M., Traversa, G., 1987. Petrological and geochemical studies of alkaline rocks from continental Brazil. 2. The Tunas massif, state of Paraná. Geochimica Brasiliensis 1, 201–234.
Gomes, C.B., Comin-Chiaramonti, P., Velázquez, V.F., Orué, D., 1996. Alkaline magmatism in Paraguay: a review. In: Comin-Chiaramonti, P., Gomes, C.B. (Eds.), Alkaline Magmatism in Central-Eastern Paraguay. Relationships with Coeval Magmatism in Brazil. Edusp/Fapesp, São Paulo, pp. 31–56.
Gomes, C.B., Dutra, C.V., Hypólito, R., Valarelli, J.V., 1968. As granadas titaníferas das rochas alcalinas de Itapirapuã, SP. Anais da Academia Brasileira de Ciências 40, 31–36.
Gomes, C.B., Moro, S.L., Dutra, C.V., 1970. Pyroxenes from the alkaline rocks of Itapirapuã, São Paulo, Brazil. American Mineralogist 55, 224–240.
Grégoire, M., Bell, D.R., Le Roex, A.P., 2002. Trace element geochemistry of phlogopite-rich mafic mantle xenoliths: their classification and their relationship to phlogopite-bearing peridotites and kimberlites revisited. Contributions to Mineralogy and Petrology 142, 603–625.
Grossi-Sad, J.H., 1972. Relatório preliminar sobre as possibilidades minerais do complexo ígneo de Chiriguelo em Pedro Juan Caballero, Paraguay Geosol, Belo Horizonte, Relatório Interno, 42 p.
Grove, T.L., Brian, W.B., 1983. Fractionation of pyroxene-phyric MORB at low pressure: an experimental study. Contributions to Mineralogy and Petrology 84, 293–309.
Haggerty, S., Mariano, A., 1983. Strontian-loparite and strontio-chevkinite. Two new minerals in rheomorphic fenites from the Paraná basin carbonatites, South America. Contributions to Mineralogy and Petrology 84, 365–381.
Hamilton, D.L., 1961. Nepheline as crystallization temperature indicators. Journal of Geology 69, 321–329.
Hamilton, D.L., McKenzie, W.S., 1960. Nepheline solid solutions in the system $NaAlSiO_4$–$KAlSiO_4$–SiO_2. Journal of Petrology 1, 1–56.
Hart, S.R., Zindler, A., 1989. Constraints on the nature and the development of chemical heterogeneities in the mantle. In: Peltier, W.R. (Ed.), Mantle Convection Plate Tectonics and Global Dynamics. Gordon & Breach, New York, pp. 261–388.
Henderson, C.M.B., Foland, K.A., 1996. Ba- and Ti-rich primary biotite from the Brome alkaline igneous complex, Monteregian Hills, Quebec: mechanisms of substitution. Canadian Mineralogist 34, 1241–1252.
Howie, R.A., Woolley, A.R., 1968. The role of titanium and the effect of TiO_2 on the cell size, refractive index, and specific gravity in the andradite-melanite-schorlomite series. Mineralogical Magazine 36, 775–790.
Kjarsgaard, B.A., Hamilton, D.L., 1988. Liquid immiscibility and the origin of alkali-poor carbonatites. Mineralogical Magazine 52, 43–55.
Laurora, A., Brigatti, M.F., Mottana, A., Malferrari, D., Caprilli, E., 2007. Crystal chemistry of trioctahedral micas in alkaline and subalkaline volcanic rocks: a case study from Mt. Sassetto (Tolfa district, Latium, central Italy). American Mineralogist 92, 468–480.
Le Bas, M.J., 2008. Fenites associated with carbonatites. Canadian Mineralogist 46, 915–932.
Livieres, R.A., Quade, H., 1987. Distibución regional y asentamiento tectônico de los complejos alcalinos Del Paraguay. Zentralblatt für Geologie und Paläontologie, Part I 7/8, 791–805.
Locock, A.J., 2008. An Excel spreadsheet to recast analyses of garnet into end-member components, and a synopsis of the crystal chemistry of natural silicate garnets. Computer Geosciences 34, 1769–1780.
Macciotta, G., Almeida, A., Barbieri, M., Beccaluva, L., Brotzu, P., Coltorti, M., Conte, A., Garbarino, C., Gomes, C.B., Morbidelli, L., Rubert, I.E., Siena, F., Traversa, G., 1990. Petrology of the tephrite-phonolite suite and cognate xenoliths of the Fortaleza district (Ceará, Brazil). European Journal of Mineralogy 2, 687–709.
Mansker, W.L., Ewing, R.C., Keil, K., 1979. Barian-titanian biotites in nephelinites from Oahu, Hawaii. American Mineralogist 64, 156–159.
Mariano, A., 1978. Report in Alkaline Rocks. Exploration in Southern PARAGUAY and Supplement on Exploration in the Area of P.J. Caballero. TAC. Asunción, Internal Report, 127 p.
Mariano, A., Druecker, M.D., 1985. Alkaline igneous rocks and carbonatites of Paraguay. Geological Society of America, Abstracts with Programs 17, 166.
Marques, L.S., Dupré, B., Piccirillo, E.M., 1999. Mantle source compositions of the Paraná magmatic province (southern Brazil): evidence from trace elements and Sr–Nd–Pb isotope geochemistry. Journal of Geodynamics 28, 439–458.
McDonough, W.F., Sun, S., 1995. The composition of the Earth. Chemical Geology 120, 223–253.
Melcher, G.C., 1966. The carbonatites of Jacupiranga, São Paulo, Brazil. In: Tuttle, O.F., Gittins, J. (Eds.), Carbonatites. Wiley, New York, pp. 169–181.
Middlemost, E.A.K., 1975. The basalt clan. Earth Science Reviews 11, 337–364.
Mitchell, R.H., 1995. Kimberlites, Orangeites and Related Rocks. Plenum, New York. 410 p.
Mitchell, R.H., Bergman, S.C., 1991. Petrology of Lamproites. Plenum Press, New York. 447 p.
Morimoto, N., 1988. Nomenclature of pyroxenes. Mineralogical Magazine 52, 535–550.
Paula, G.S., 2004. Estudos petrográficos, geoquímicos e geotectônicos do magmatismo alcalino Eocretáceo da Província Amambay, nordeste do Paraguai Oriental. Graduate Dissertation, Institute of Geosciences, University of São Paulo, 62 p.. (unpublished).
Putirka, K., 1999. Clinopyroxene + liquid equilibria to 100 kbar and 2450 K. Contributions to Mineralogy and Petrology 135, 151–163.
Ruberti, E., 1984. Petrologia do maciço alcalino do Banhadão, PR. Ph.D. Thesis, Institute of Geosciences, University of São Paulo, 248 p. (unpublished).
Ruberti, E., Gomes, C.B., Comin-Chiaramonti, P., 2005. The alkaline magmatism from Ponta Grossa Arch. In: Comin-Chiaramonti, P., Gomes, C.B. (Eds.), Mesozoic to Cenozoic Alkaline Magmatis in the Brazilian Platform. Edusp/Fapesp, São Paulo, pp. 472–521.
Sato, K., Tassinari, C.C.G., Kawashita, K., Petronilho, L., 1995. O método Sm–Nd no IG/USP e suas aplicações. Anais da Academia Brasileira de Ciências 67, 313–336.
Shaw, C.S.J., Penczak, R.S., 1996. Barium- and titanium-rich biotite and phlogopite from the western and eastern gabbro, Coldwell alkaline complex, northwestern Ontario. Canadian Mineralogist 34, 967–975.
Sonoki, I.K., Garda, G.M., 1988. Idades K/Ar de rochas alcalinas do Brasil meridional e Paraguai oriental: compilação e adaptação às novas constantes de decaimento. Boletim do Instituto de Geociências da USP,Série Científica 19, 63–85.
Sørensen, H., 1960. On the agpaitic rocks. In: International Geological Congress, 21, Norway, XXI Session, Part XIII, pp. 319–327.
Spinelli, F.P., Gomes, C.B., 2009. A ocorrência alcalina de Cananéia, litoral sul do Estado de são Paulo: química mineral. Geologia USP, Série Científica 9, 1–13.
Thiede, D.S., Vasconcelos, P.M., 2008. Paraná flood basalts: rapid extrusion hypothesis supported by new $^{40}Ar/^{39}Ar$ results. In: 44° Congresso Brasileiro de Geologia, Curitiba, Províncias Magmáticas: magmatismo básico-ultrabásico, p. 563.
Tilley, C.E., 1954. Nepheline-alkali feldspar parageneses. American Journal of Sciences 252, 65–75.
Traversa, G., Barbieri, M., Beccaluva, L., Coltorti, M., Conte, A.M., Garbarino, C., Gomes, C.B., Macciotta, G., Morbidelli, L., Ronca, S., Scheibe, L.F., 1996. Mantle sources and differentiation of alkaline magmatic suite of Lages, Santa Catarina, Brazil. European Journal of Mineralogy 8, 193–208.
Wiens, F., 1991. Exploración mineral en Paraguay Oriental Report Geoconsultores, Asunción, Paraguay, 298 p.
Wyllie, P.J., 1995. Experimental petrology of upper mantle materials, processes and products. Journal of Geodynamics 20, 429–468.
Zhang, M., Suddaby, P., Thompson, R.N., Dungan, M.A., 1993. Barian titanian phlogopite from potassic lavas in northeast China: chemistry, substitutions, and paragenesis. American Mineralogist 78, 1056–1065.